FIRE SIMULATION AND ANALYSIS OF A SWITCHGEAR CABINET FIRE AND ITS EFFECTS ON CABLE TRAYS

A Thesis Presented for the

Master of Science

Degree

The University of Tennessee, Knoxville

Yalcin Meraki

August 2022

ACKNOWLEDGEMENTS

Thank you to Dr. Eric D. Lukosi for his support and guidance during my graduate education and thesis studies. Thank you to Dr. David Icove for teaching me some fire analysis and protection software programs. Thank you to Dr. G. Ivan Maldonado for giving feedback and serving on my thesis committee. Finally, thank you to the Turkish Ministry of National Education for providing me with the opportunity of studying abroad by supporting me financially.

ABSTRACT

Switchgear rooms are crucial in containing essential equipment such as cabinets and cable trays in case of a possible fire. There are three fire model classes which are algebraic models, zone model, and computation fluid dynamics model (CFD). PyroSim software, a visual user interface for the Fire Dynamics Simulator (FDS) developed at the National Institute of Standards and Technology (NIST), was used for simulation by using the CFD. Two different 464 kW and 1002 kW heat release rate (HRR) values were used under the same conditions for the fire scenario. By considering a fire scenario, the fire ignited due to an electrical fault in bundles of PE/PVC cables in the cabinet. In addition, this fire modeling scenario determined whether the cabinet fire caused any secondary fires in the other side cabinets or the horizontal cable trays above the cabinets and at what time these secondary fires occurred.

TABLE OF CONTENTS

LIST OF TABLES

LIST OF FIGURES

Chapter 1 Introduction Nuclear Power Plants and Nuclear Fire Safety

Nuclear power plants are complicated. They have many different systems designed to work well in both usual and unusual situations. A nuclear power plant must handle a considerable amount of energy while keeping everyone very safe. All of the system's functions must be controlled in a way that guarantees their operation and reliability. The equipment used must hold up over time despite being exposed to extremes of temperature, pressure, humidity, radiation, vibration, and shaking, such as from earthquakes [1].

Uncontrollable fires in nuclear power plants pose a significant threat to facility safety. Since a fire that damages some of these systems could make it unsafe for a nuclear power plant to run. In recent years, the Nuclear Regulatory Commission (NRC) has given much thought to figuring out how well power plant fire protection works. As a result, the Nuclear Regulatory Commission (NRC) has initiated a wide-ranging research program in fire protection, a significant amount of which focuses on the conduct of fire-hazards evaluations. Some of this attention has been given in the form of rules and regulations right after the Browns Ferry Fire in 1975. Other work has been done with the long-term aim of understanding how fires happen in nuclear power plants [1], [2].

Combustion is a chemical reaction that occurs due to the combination of flammable materials with heat and oxygen under appropriate conditions. On the other hand, fires the combustion event in which these mergers occur involuntarily [3].

Many of the combustible materials in nature are fossils with organic compounds. If there is a high temperature in any environment and sufficient oxygen for combustion in the same environment, the combustion of all materials can be achieved. There are Carbon, Sulfur, Phosphorus, and Hydrogen in the structural combinations of combustible materials. Combustible materials exist in nature in three forms: solid, liquid, and gas. Oxygen is a colorless and odorless gas that does not show combustion but causes

combustion. The air in a clean environment contains 20% oxygen under ideal conditions. In cases where the oxygen rate does not fall below 16%, combustion occurs. If it falls below this rate, the burning starts to go out. If it falls below 14%, explosion does not occur [4].

Not taking fire protection measures or not taking care of the equipment on time, not using appropriate materials, negligence, natural events, accidents, and carelessness are the most common causes of fire [5].

The primary purpose of the fire is to prevent the formation of smoke. Because smoke is the most important cause of loss of life due to fire. For this, the materials used in the design phase should be selected from materials resistant to combustion or do not emit harmful gases. For example, using halogen-free, non-flammable cable instead of halogen cable will prevent toxic materials that may occur in fires that may arise from electrical panels. Halogen materials fluorine, chlorine, bromine, etc., contain harmful chemicals. Apart from this, structural measures such as building architecture, determination of escape routes, and creation of fire compartments should be taken. Despite all these precautions, it is necessary to direct the smoke and make evacuation programs without harming people against a fire that may occur. So that, the most prominent cause of death from fire is loss of life due to gases and fumes, accounting for 45% of all fire-related deaths [6].

1.1 The Fundamentals of Fire

1.1.1 Fire and Flame

The fire of a substance releases heat, light, and various reaction products. Other oxidation processes, such as rusting and digesting, are not discussed. The flame is the visible part of the fire and is made up of burning hot gases. The gases may get ionized

and form plasma if heated sufficiently. The color and intensity of the flame vary depending on the materials that are burning, and any particles present outside. Conflagration is the most common type of fire, and it has the capacity to cause bodily harm by burning[7].

Fires begin when a flammable or combustible substance is exposed to a source of heat or an ambient temperature that is greater than the material's flash point, in combination with an oxidation environment that is conducive to sustaining a chain reaction for fast oxidation[8].

1.1.2 Fire Triangle

For ignition and combustion to occur, three components, heat, oxygen, and fuel, must be present in a particular combination. This is known as the fire triangle, as seen in figure 1. If any of the three are missing or out of equilibrium, ignition or combustion cannot occur. Variations in heat, oxygen, and fuel balance influence the intensity of a fire and decide whether it will smoke and develop slowly or flame brightly and spread quickly. All these components must be present and in the proper amounts for fire to exist.

The fuel component of this fire triangle might be solid, liquid, or gas. However, solid, or liquid fuels must be heated sufficiently to evaporate before they can be burned. Therefore, this triangle's oxygen and heat components must be sufficient to allow for fast oxidation. Different fuel sources will typically require oxygen and heat variables[8].

1.1.3 Fire Phases

The burning process is divided into distinct stages. When a firefighter identifies the various stages, he or she can better comprehend the process of burning and controlling the fire at multiple stages, using different tactics and instruments. Differences in room temperature and air composition describe each stage. The steps are graphically indicated in Figure 2 below.

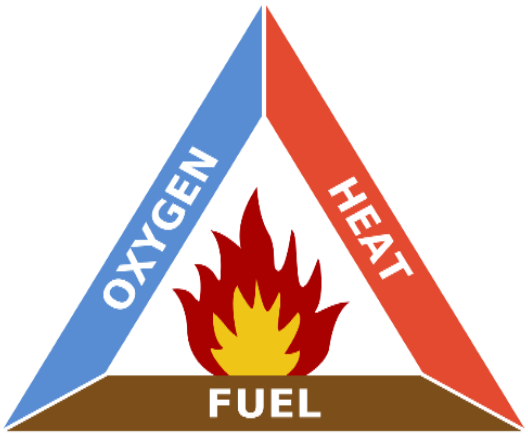

Figure 1: Fire Triangle[8]

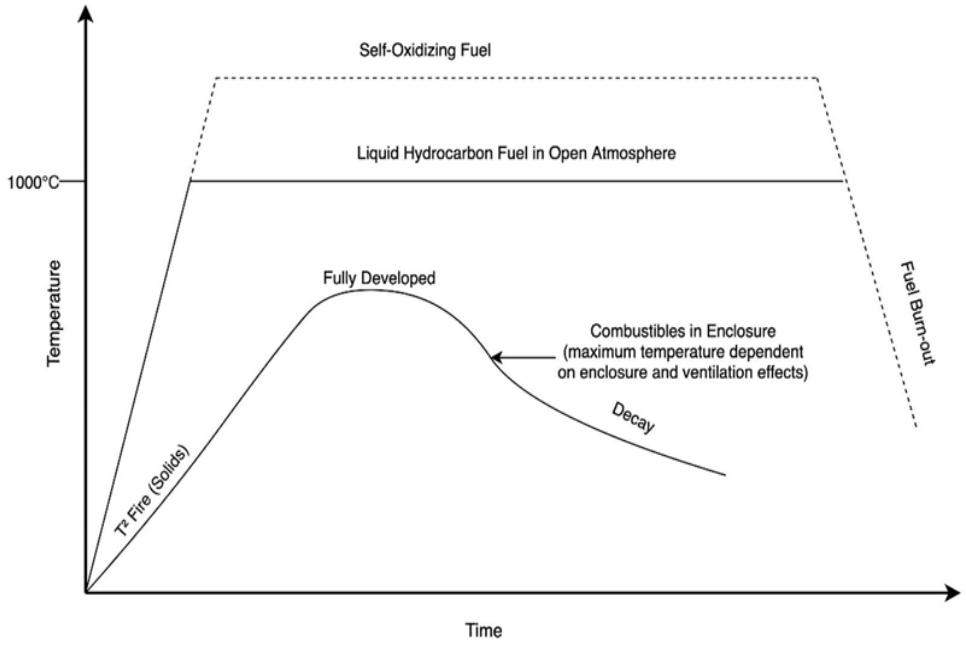

Figure 2: Fire development parameters for solid, liquid, and self-oxidizing fuels in general [9]

The incipient stage of fire growth is often confined to a specific fuel source because the heat created cannot transmit enough heat to neighboring fuel sources for combustion. The following phase happens when the incipient fire has become large enough that the heat transfer to close adjacent fuel sources is large sufficient to pyrolyze them, causing fire expansion. The highest fire temperature would be restricted by the size of the enclosure and the impacts of ventilation. A flashover phase may occur in certain circumstances, but not all. A flashover happens when all the surfaces within the container are exposed to enough thermal radiation from the fire for simultaneous ignition and full room involvement. Whether or not there is a flashover, the fully developed phase occurs when the peak heat release rate of the combustibles in the compartment is reached. The last step is the decline phase, which occurs when the fuel load in the room begins to diminish, or the amount of available oxygen to sustain combustion is achieved[10].

1.1.4 Product of a fire

It is a chemical process that is unique to each type of material that is burned quickly. As soon as a combustible material starts to get hot, the material given to it must be changed into something that can be pyrolyzed or evaporated. When a fuel is burned, there are four products that happen: fire gases, heat, flame, and smoke. Most fire gases are made up of oxygen, nitrogen, carbon dioxide, carbon monoxide, and small pieces of carbon. These gases could spread the fire and have toxic effects on people who are near the fire. Flames and the heat and smoke that come from a fire are the main things that can damage equipment and people.

In this thesis, the expected fire scenario in the switchgear room is the first cabin fire and secondary fires of the cable trays on the cabinets due to this fire. For the purposes of this fire modeling, determine if any cabinet fires are causing secondary fires in other cabinets or horizontal cable trays above cabinets. This study aims to look into this situation and determine if these targets fail and, if so, when the failure occurs. PyroSim

program is a graphical user interface for version 6.7.4 of the Fire Dynamics Simulator (FDS) is used for this fire modeling.

1.2 Significant Fires in The Past

1.2.1 1975 Brown's Ferry, The U.S.A.

On March 22, 1975, a fire broke out at the Browns Ferry Nuclear Power Plant near Decatur, Alabama. The Special Investigation Team was deployed immediately after the fire by the Nuclear Regulatory Commission's Directorate-General for Operations (NRC) to determine the causes of this event and make recommendations for the future based on this data.

In this reactor, there is a cable distribution room just below the control room. The Browns Ferry facility consists of three boiling water reactors, each designed to generate 1067 MeV electricity. Units 1 and 2 are active at the time of the fire, while unit 3 is still under construction. The most significant cause of the fire was the ignition of the polyurethane foam used for insulation.

The fire occurred in the wall section between the cable distribution room and the Unit 1 reactor building. The fire was extinguished with the installed carbon dioxide extinguishing system and manual fire extinguishing efforts [11].

1.2.2 1975 Greifswald, Germany

In December 1975, a fire broke out in the 6 KeV switch room in Unit 1, which was put into operation in December 1973. According to one of the reports on the fire, due to the fault of an electrician, a high current flowing through the wires for several minutes

led to a short circuit, followed by failure of the automatic circuit breakers. The fire lasted close to 1.5 hours and destroyed most of the cables [12].

1.2.3 1979 Barseback, Sweden

Ignition occurred due to oil leakage because of breakage in turbine blades. The ejected particles hit the nozzles in the sprinkler system, and the fire spread around, affecting other systems [11].

1.2.4 1993 Narora, India

The fire in the turbine building of Narora Atomic Power Station (NAPS) Unit 1 caused 17 hours of power loss. In the accident, a severe imbalance occurred in the turbo generator because of the failure of two turbine blades in the last stage of the low-pressure turbine and the hydrogen gaskets and engine oil lines that broke off as a result of this imbalance caused a fire. The fire spread to components such as many cable ducts and relay panels quickly. Using the first stop system with manual triggering, the operating team abruptly stopped the reactor and started the rapid cooling process. The fire spread to the equipment control room through the generator distribution channel and cables inside the turbine building. Smoke filled the control room through the ventilation system, forcing the operators to evacuate the room. The spare indicators in the supporting control room have also become unusable due to the burning of the control cables. Extensive damage occurred to the power cables as well as the control cables [11].

1.2.5 1995 Waterford, The U.S.A.

In Waterford, this reactor has a PWR-type design. The minor accident in the main switch room had little effect on safety functions. Primary switch fires are among the most

common fires in an NPP. One of the points of interest due to the accident is what happened to the main switch cabinet and the wiring on the cabinet. Three cabins were severely damaged, and the fourth suffered minor damage. Moreover, the fire was not blocked by any fire barrier until it spread through the steel panel to the vertical cable tray, from there to another vertical tray 3 meters above and a horizontal channel 2.5 meters away. The potential to spread to the outside in closed electrical panels has not been so significant until now. However, this accident clearly demonstrated the existence of such a possibility.

Another remarkable detail is that the fire damage reaches the neighboring cabins. Only two adjacent cabinets were severely damaged in the accident, while the other four suffered superficial damage. This situation increases the possibility that the person inspecting the related field has ignored the heat transfer with radiation [11].

Chapter 2 Fire Modeling Theory

In compartments, fire growth is frequently split into phases based on the primary processes at each stage of development. The parameters of the fuel being ignited (i.e., ignition temperature, structure, orientation, and thermo-physical properties) and the intensity of the ignition source govern ignition[13]. As a result of the smoke's buoyancy, mass and heat are transported upward after the flames are maintained on a burning fuel item, and a smoke plume form, as seen in Figure 1.

As the plume rises, it will take in air, causing the smoke to cool and get diluted; hence, the amount of smoke delivered will increase with height. A ceiling jet is a relatively thin layer of smoke that runs horizontally under the ceiling when a smoke plume impacts the ceiling. As the ceiling jet spreads, soot cools with increasing distance from the plumes point of impact, due partly to air entrainment into the ceiling jet and heat loss from the ceiling jet to the solid ceilings border[13].

A Hot Gas Layer (HGL) in an ideal setting occurs after the ceiling jet reaches the surrounding walls. As a result of the plume's continued supply of smoke mass and heat, the HGL grows in depth and temperature. Additionally, other qualities of the smoke in the HGL increase (includes gas species concentration and solid particle concentration).

Radiant heat from the HGL enhances the temperature of combustibles that are not involved in the fire. Similarly, non-combustible combustibles will cause a rise in temperature due to receiving thermal radiation from burning objects. The other combustibles will ignite when they reach their target ignition temperatures. In certain instances, the warmth from the HGL causes the rapid ignite of a large number of additional combustibles in the area. This condition is generally known as flashover[6].

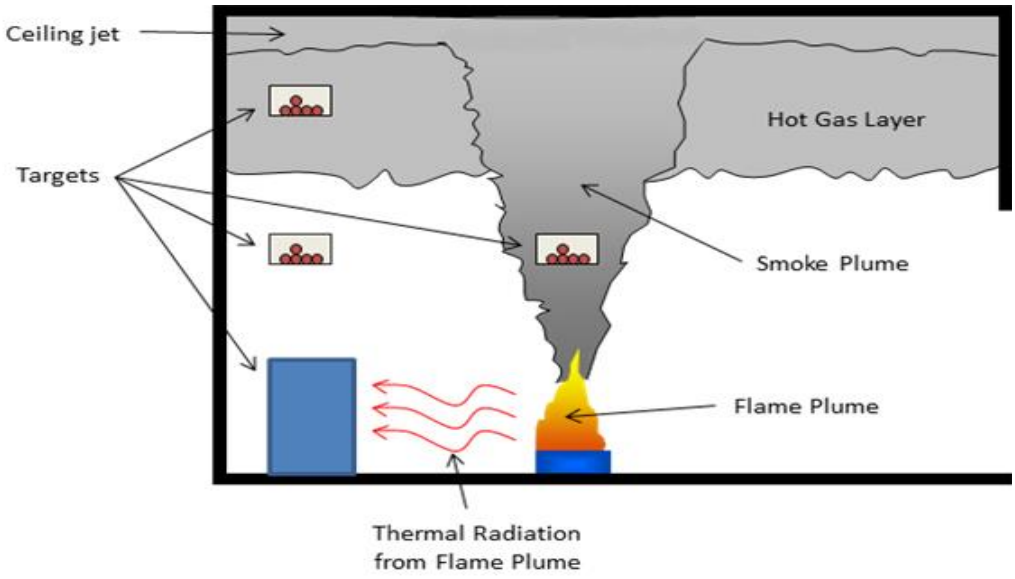

Figure 3: Components of compartment fires[13].

2.1 Fire Modeling Tools

There are three fire model class which are algebraic models, zone model, and computation fluid dynamics model. In this study, CFD is used, which provides detailed fire modeling in complex geometries. The advantage of using this model is the ability to simulate fire conditions in complex geometries and with complex vent conditions. However, it takes long simulation times. The mass, momentum, and energy conservation equations are basically solved using CFD models on a computational mesh.[14]

2.1.1 Algebraic Models

Algebraic models are equations that can be found in books or in spreadsheets (like the NRC's FDTs). They can help us get a general idea of how one of the fire environment phenomena works. Closed-form algebraic expressions make up the majority of these equations., and a lot of them were made by finding correlations between actual data. In some cases, they may look like equation of the first order of ordinary differential. However, when used correctly, they can give an estimate of fire variables like HGL temperature, heat flux from flames or the HGL, rate of smoke emission, the HGL's depth, and the time it takes for detectors to go off.

Hand calculation models are advantageous since they need minimum processing time and few input variables. However, when using the findings of algebraic models, users must be aware that approximations were used to generate the majority of equations to simplify the analysis[10].

2.1.2 Zone Models

Consolidated Fire Growth and Smoke Transport Model (CFAST) or MAGIC software are two examples of zone models. These variables of the environment are

calculated based on control volumes, or zones, of a given area. Each zone is well-mixed in a zone model, and all factors in the fire environment are taken into account (temperature, soot concentration, etc.) are consequently uniform across the zone. By utilizing conservation equations and the ideal gas law, the conditions of each zone are computed. The variables in each area vary as a time function and depend on the user-specified beginning circumstances. There is a well-defined border between the two zones, although this barrier may rise or fall as the simulation progresses.

Zone models make it easy to look at the effects of fires in single compartments or in compartments that are next to each other. They are frequently used to determine the HGL's temperature, composition, and required heat fluxes. In both horizontal and vertical lines, they can also simulate some of the impacts of natural and mechanical ventilation[10], [13].

2.1.2 Computational Fluid Dynamics (CFD) Models

When attempting to determine fire variables at a given site or when geometric components are predicted to play a larger influence in the outcomes than can be approximated by a zone model, a computational fluid dynamics (CFD) technique is typically useful. Both simple and complicated geometries can be analyzed in detail with CFD models[15]**.**

Many conservation and state equations are applied across many cell borders in a space in CFD models. The mesh size, which divides the geometry into three-dimensional sub volumes called cells, determines the number of cell borders. Inside each numerical grid cell, solutions to the mass, momentum, and energy conservation equations are adjusted as a function of time, with the solutions in all cells cumulatively characterizing the fire environment inside the geometry at the scale of individual cells[10].

The kind of mesh is determined by the number of grid cells. A fine mesh is composed of several grid cells. Due to applying the equations at each cell's boundary, a more exact distribution of fire parameters is defined. A coarse mesh consists of fewer grid cells and may produce a less accurate result. The geometry and intended outcomes must determine the kind of mesh and number of grid cells 16].

Depending on how complicated the situation is and how fast the computer is, the model's solver could take anywhere from a few hours to a few weeks to finish all the calculations. The amount of time this will take depends on the parameters that were measured, the geometry size, and the calculations' mesh size. A post-processing application is used to display the results of CFD models. Fire Dynamics Simulator (FDS), a CFD model created by NIST, uses the application "Smoke view" to simulate distributions of temperature, mass, heat flux, burning rate, etc., across the geometry[10].

CFD models are useful for calculating the time to fire detection in complicated geometries, especially those with obstacles, since they can precisely characterize the complex geometries and mechanical ventilation conditions of the compartment[17].

2.2 The Fire Dynamics Simulator

The National Institute of Standards and Technology (NIST) creates and maintains the FDS. Simulation software is the basis for the FDS model of fire-driven fluid flow (CFD). The approach computationally resolves a variant of the Navier-Stokes equations based on low, thermally driven flow, with a focus on heat and smoke transfer from fires. The technique is time-based and three-dimensional, rectangular shapes grid, and the partial derivatives of the mass, momentum, and energy conservation equations are roughly represented as discrete disparities. On the same grids as the flow solver, thermal radiation is calculated by using appropriate boundary conditions. The simulation of soot and sprinkler sprays which are using Lagrangian particles. Smokeview is an additional application that generates visuals and animations of FDS computations[18].

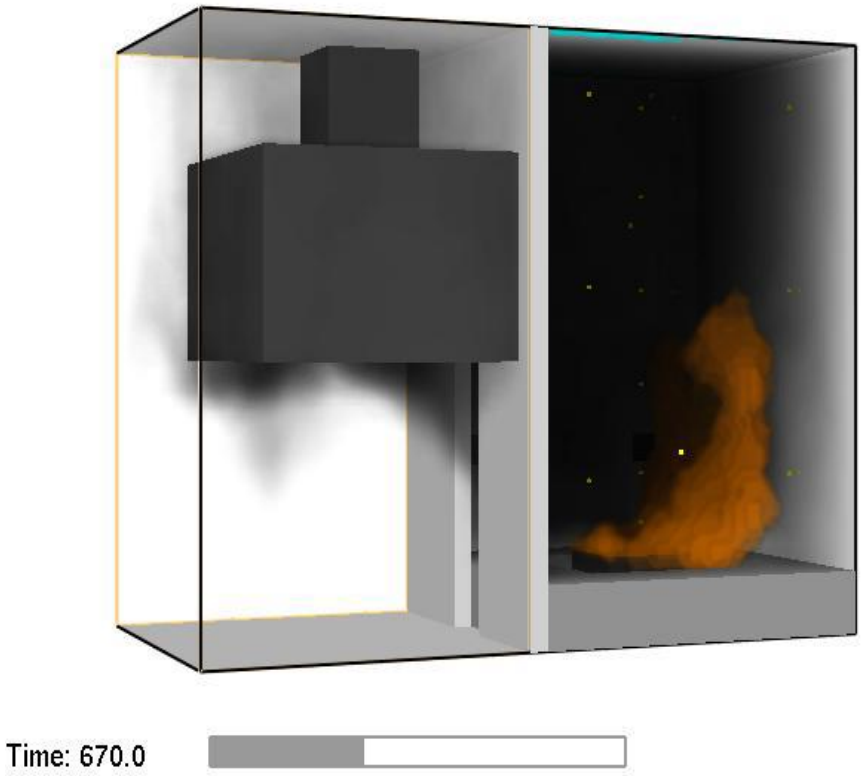

Figure 4: A Smokeview display of a compartment fire experiment CFD model[10]

2.3 An Overview of PyroSim

PyroSim software is a graphical user interface for version 6.7.4 of the Fire Dynamics Simulator (FDS). Both these software's are deeply linked. During a fire, FDS models can predict how much soot, carbon monoxide, and other chemicals will be in the air. The findings of these simulations are used to check building safety before construction, evaluate current building safety alternatives, rebuild fires to investigate accidents, and help in firefighter training[19].

2.3.1 Property Libraries

PyroSim offers parameter property libraries for model parameters, such as construction materials, pyrolysis activities, combustion particles, sensor systems, etc. In general, the pre-defined material libraries are enough for learning the program or training others. Still, they are insufficient when doing academic research or evaluating the fire resistance design of a structure. Nevertheless, the property libraries describe the model parameters for usage with FDS, improving its usability and accelerating model construction. Users are able to directly load the predefined libraries and create/delete libraries as required. Figure 5 demonstrates how to access the materials library[20].

2.3.2 Post-processing

The SMV software in the FDS model is developed for viewing the fire as a dynamic 3D animation, and dynamic 2D fire data may be added to the Static program as XY time history plots. PyroSim includes post-processing simulation outputs that let these visualizations to be initiated at any moment during analysis as seen Figure 6. Consequently, users may regularly access the findings to examine, evaluate, or even cancel the created situation if they are dissatisfied with the outcomes, which increases simulation efficiency and time savings[20].

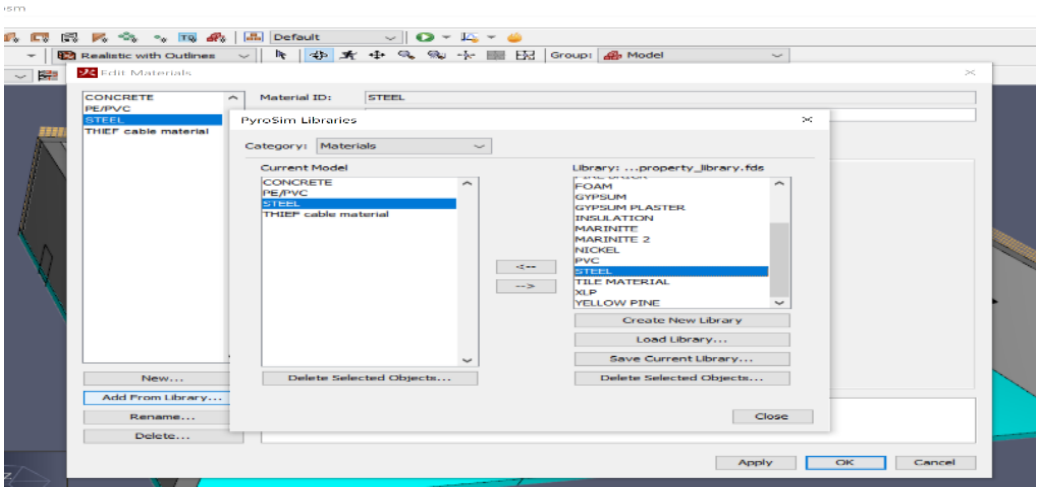

Figure 5: Loading the Steel material property from the libraries

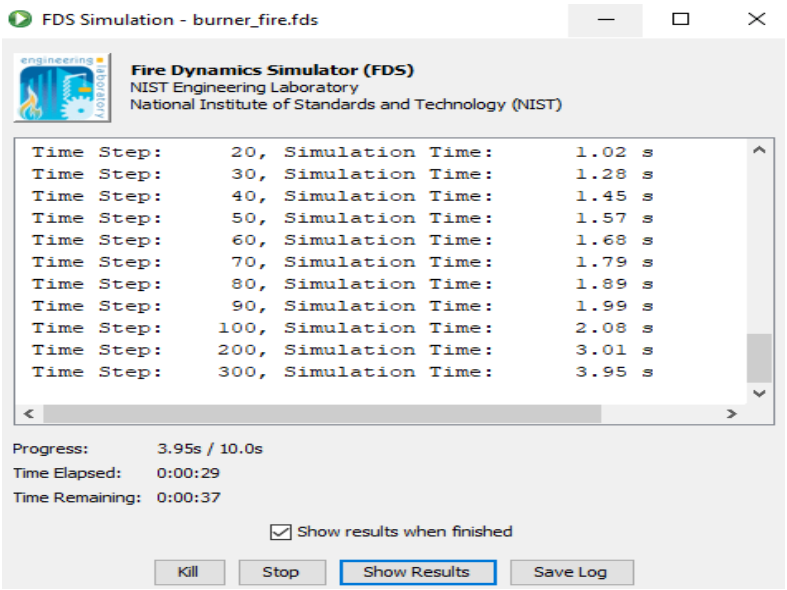

Figure 6: While a model is being worked on, the results can be shown[20]

2.3.3 Model Results

For each discrete time period, FDS determines the temperature, pressure, velocity, density, and chemical make-up of each grid cell. It is typical to use a few hundred thousand to several million grid cells as well as a few thousand to tens of thousands of time steps. In addition, FDS calculates the heat flow, temperature, and mass-loss rate at solid surfaces, among other characteristics. The user must carefully choose which data to keep, similar to how one would construct an experiment. Even though only a tiny fraction of the calculated information may be stored, the output is often comprised of quite big data files[20]. Typical gas phase output amounts include the following:

- Gas velocity
- Gas temperature
- Pressure
- Heat release rate each unit of volume
- Temperatures at the surface and depth
- Burning rate
- The mass of water droplets per unit area
- The rate of total heat loss

Smokeview, a tool mainly intended to evaluate data produced by FDS, is used to display most field or surface data. To simulate and display fire phenomena, FDS and Smokeview are utilized together. Smokeview shows this visualization's animated tracer particle flow, updated contour slices of calculated gas variables, and updated surface data. Smokeview also displays outlines and vector plots of static data at a specific moment anyplace inside a field[19].

2.3.4 Grid Size

In FDS, the size of the grid cells is the most crucial number. On a grid of numbers, CFD models solve an approximation of the equations that describe how mass, momentum, and energy stay the same. The size of the grid cells and the kind of differencing utilized affect the inaccuracy introduced by discretizing partial derivatives. FDS gets close to the second-order derivatives of the Navier-Stokes equations for both time and space. This means that the error in discretization is equal to the square of the size of the cell. In principle, it is lowering the grid cell size by a factor of two results in a reduction in discretization error that is equal to a factor of four. On the other hand, this results in a 16-fold increase in the amount of time required for computation (a multiplicative factor of 2 for both temporal and spatial dimensions). A grid sensitivity study is a kind of research that is used to determine what size grid cell should be used in a certain computation[18].

The grid sizes are computed using the characteristic diameter of the fire and grid size ratio, which, based on the overall heat release rate, should appropriately resolve our fire simulation. The typical fire diameter (D*) may be connected to the cell size (dx) for a specific simulation. This means that the smaller the characteristic diameter of the fire, the smaller the grid size need to be in order to appropriately resolve the fluid flow and fire dynamics.

The following relationship gives the characteristic fire diameter (D*):

$$D^* = \left(\frac{Q}{\rho_\infty c_p T_\infty \sqrt{g}} \right)^{\frac{2}{5}}$$

Where Q represents the heat release rate, ρ_∞ represents the ambient density, c_p defines the specific heat, T_∞ represents the ambient temperature, and g is the acceleration of gravity. FDS models the unresolvable or "sub-grid" motion of the hot

gases using a numerical approach which is called "Large Eddy Simulation" (LES).The technique's efficiency is primarily determined by the proportion of the fire's characteristic diameter, D*, to the size of a grid cell, dx. The bigger the ratio D*/dx, the better the direct resolution of fire dynamics and the more realistic the simulation. The past experiences have shown that a ratio of 5 to 10 yields excellent outcomes at a low computational expense[18]. The FDS User Guide NUREG 1824 referenced a D*/dx ratio between 4 and 16 to properly resolve fires in a variety of conditions.

Figure 7, for instance, shows the plume temperature forecasts for Test 5 of the FM/SNL series, calculated on a 10 cm, 7.5 cm, and 5 cm grid. A simulation of 10 cm requires many hours to execute on a 2.4 GHz Pentium CPU, but the simulation of 5 cm takes many days. The prediction is much more accurate for the 5 cm grid because the absorption of air into the hot plume is described with higher precision.

2.3.5 The Heat Release Rate (HRR)

The heat release rate (HRR) is expressed as the ratio during which the combustion process releases heat. Among the parameters used in determining fire consequences, the heat release rate (HRR) is perhaps the most critical and challenging to predict. This is due to the fact that the HRR serves as the driving parameter for evaluating conditions in fire-induced flows such as plumes, ceiling jets, soot layers, and radiation from flames.

Typically, the HRR is determined using the combustibility characteristics of the fuel. This approach is easily applicable to flammable liquids and certain plastics. These flammability measurements are the heat of combustion (ΔH_c, kJ/kg) and the specific burning rate ($\dot{m}''$, kg/secm^2). Using these two factors and the burning area, the HRR is estimated as follows:

$$\dot{Q}_f = \Delta H_c . \dot{m}'' . A$$

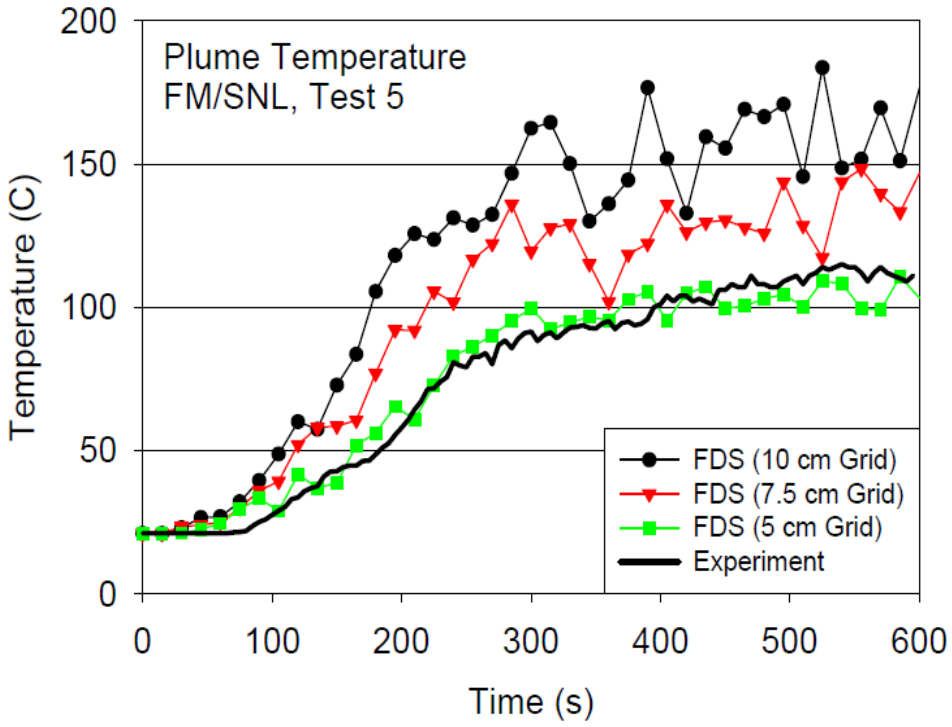

Figure 7: Grid sensitivity study[18]

In practical applications, the HRR is separated into stages of the fire. These stages are incipient, growth, fully developed, and decay, as seen in Figure 8. In the stage of incipient, the fire burns with modest intensity. This phase's length might range from seconds to hours. Under optimal conditions, an incipient fire might reach its maximum HRR. Depending on the combustible and its structure, the time required for a fire to reach a fully grown stage might range from seconds to minutes. Based on the quantity of fuel and the amount of oxygen around the combustion process, a fully grown fire will burn. As fuel is spent, the HRR profile will enter the decay phase. If there is insufficient oxygen to support the reaction, the fire will also diminish in intensity[13].

These four phases are not present in all fires and do not need to be accounted for in every analysis, so long as the modeled fire conditions transmit the fire hazards posed by the ignition source to the target. Combustible room design can have an effect on HRR profiles. Therefore, it is not always simple to design or locate a profile for a particular circumstance. If a uniform HRR profile is used, the constant value will be the highest fire level. In general, the temperature and heat flow values connected with the decay stage of the fire will indicate less dangerous conditions than those associated with the fully grown stage. Once the fire begins to go down, the room temperature will return to normal. Consequently, and depending on the aims of the simulation, simulating the decaying phase of the fire typically does not give crucial information to support risk assessments[13]. Table -1 shows the recommended HRR values for cables.

The following HRR profile is suggested for electrical cabinets:

- The fire reaches its maximum HRR in around 12 minutes.
- The fire maintains its maximum heat output for another eight minutes.

A t^2 the function can be used to represent the fire's growth phase. The t^2 the function has the following formula:

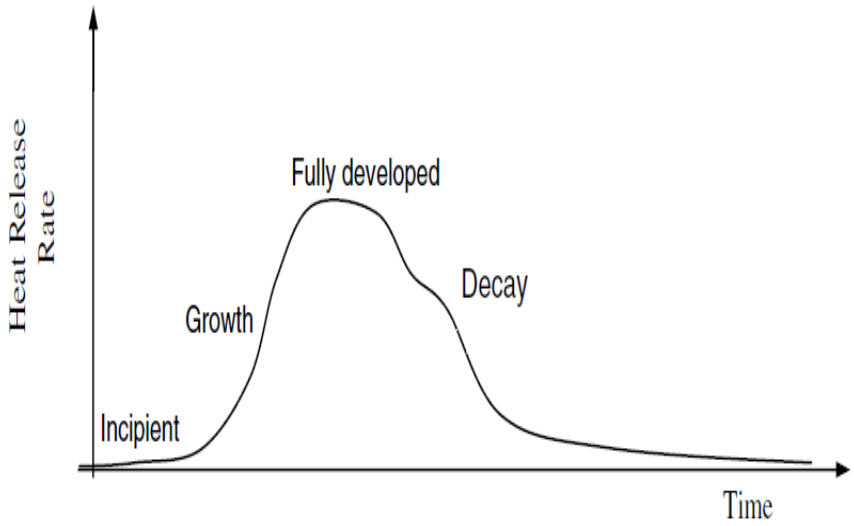

Figure 8: Profile of Heat Release[13]

Table 1: Recommended HRR Values for Electrical Fires[13].

Ignition Source	HRR (kW)
The fire is confined to one cable package in vertically cabinets with certified cable.	211
Fire in several cable bundles in vertical cabinets equipped with certified cable.	702
There are vertical cabinets with unqualified cable, and the fire is localized with one cable package per cabinet.	211
Unqualified cable, fires in more than one cable package, and closed doors in vertical cabinets	464
Fire in more than one cable package opens the doors of vertical cabinets with unqualified cable.	1002
Pumps	211
Motors	69
Transient Combustibles	317

$$\dot{Q}(t) = Min\left\{\dot{Q}_{peak}, \dot{Q}_{peak}.\left(\frac{t}{\tau}\right)^2\right\}(kW)$$

$\dot{Q}_{peak}$ is peak HRR, t is time, and T represents the time to reach the peak HRR.

2.3.6 Particle Clouds

Particle clouds allow particles to be inserted into the simulation in a box-shaped region or at an exact position. Either particles exist at the beginning of the FDS simulation, or they are regularly added[19].

Chapter 3 Fundamentals of Electrical Cables

The role of an electrical cable is to provide a medium for conveying electrical energy between two places in a single electrical circuit while simultaneously isolating the transmission channel from other parts of the same switch and other co-located connections. Therefore, cable failure means a lack of continuity in the energy transmission line or the diversion of a substantial portion of the available electrical energy to an unanticipated circuit destination such that the circuit's regular operation is no longer possible. Hundreds of kilometers of electrical cable are commonly found in nuclear power plants[8]. A typical boiling-water reactor (BWR) needs 97 kilometers (60 miles) of power cables, 80 kilometers (50 miles) of control cable, and 400 kilometers (250 miles) of instrument cable. More cables may be required for a pressurized-water reactor (PWR)[21]. In addition, most fire dynamics and fire risk studies focus on electrical wires due to their thermal fragility. Therefore, a basic knowledge of electrical cables is required for doing fire simulation and analysis.

Several types of cable failures can be caused by a fire. Different forms of fire-induced failures in electrical cables can cause a variety of circuit faults, resulting in diverse circuit faulting behaviors, as demonstrated by actual fire incidents[8].

3.1 Construction of Electrical Cables

Cables are available in a vast array of combinations. The critical configuration features that characterize a specific cable are the conductor size, the number of conductors, shielding features, and insulation/jacket materials.

Thermoplastic and thermoset materials are the most complete types of materials that may be used as cable insulation and jacketing. Thermoplastic materials melt at high temperatures and solidify at low temperatures. If heated sufficiently, thermoset materials

start to smolder and catch fire instead of melting. Thermoset materials generally are more durable, with failure temperatures greater than or equal to 350 °C (662 °F). The failure temperatures of thermoplastic materials are often significantly lower than 206 °C (420 °F), when failure is typically linked with the melting of the material[22]. Typical thermoset cables burn at a rate of approximately 150 kW/m2, and standard thermoplastics burn at a rate of around 250 kW/m2, as shown in Figure 9.

Typical cable components include one or more metallic conductors, insulation, shielding, sheathing, and jacket. Insulation covers each metallic conductor, which is often copper or aluminum, to provide electrical isolation. Insulation, which is sometimes regarded as the essential component of a cable, is generally composed of a dielectric substance such as plastic and rubber. Typically, cable jackets are composed of rubber or plastic. The goal of the jacket is to give physical or environmental protection and enhanced flame retardancy to the insulated conductors. Cable jackets with improved flame retardancy limit the propagation of flame over the jacket and minimize the cable's fuel contribution once ignited. However, greater flame retardancy does not guarantee functioning[8].

Overall, insulation is crucial to the overall functioning of a cable at normal and increased temperatures. Insulation serves to electrically isolate each conductor from the other conductors and the ground plane.

3.2 Thermoplastic Materials

Thermoplastic materials are described as polymers with a high molecular weight that are not cross-linked and are often distinguished by the insulating material's specific melting point. The physical attribute of thermoplastic materials is that they may be repeatedly softened by heating and toughened by cooling within a temperature band. This feature is a result of the material's loose molecular bonds. Several thermoplastic materials have a low melting temperature, which can be a negative since insulation melting at

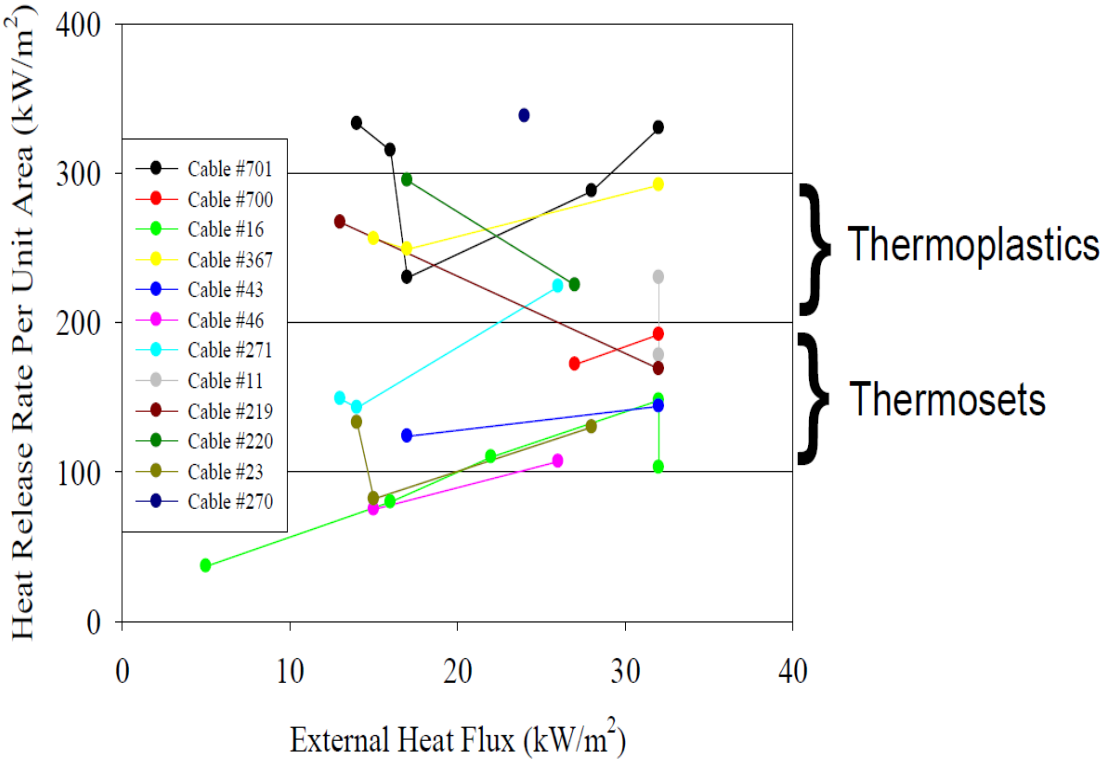

Figure 9: Thermoplastics and thermosets the radiant panel heat release rates[23]

Table 2: Damage Threshold for Electrical Cables

Cable Type	Heat Flux Criteria	Temperature Criteria
Thermoplastic	7 (kW/m^2)	206 (°C)
Thermoset	11 (kW/m^2)	350 (°C)

relatively low temperatures can cause conductor problems. Thermoplastic insulation is typically simple to make and cost-effective to utilize[21]. Examples of thermoplastic types are low and high polyethylene (PE), polyvinyl chloride (PVC), polyurethane, polypropylene (PPE), nylon, chlorinated polyethylene (CPE), and Teflon. The suggested failure threshold for the general class of thermoplastic cables is 420 °F (206 °C).

3.3 Thermoset Materials

The molecular network is made up of chains that are connected by covalent bonds (crosslinked). When exposed to higher-than-normal temperatures, thermoset insulation weakens but does not melt. While they weaken, they tend to keep the insulator's mechanical qualities. As a result, thermoset insulations outperform thermoplastic insulations in terms of low- and high-temperature characteristics, thermal aging resistance, and overload resistance. Examples of thermoplastic types are ethylene-propylene rubber (EPR) and crosslinked polyethylene (XLPE). The suggested failure threshold for the general class of thermoset cables is 662 °F (350 °C), as seen in Table-2 [21].

Chapter 4 Verification and Validation Parameters

4.1 Froude Number

The Froude Number quantifies the height of a fire plume. A high Froude Number indicates a powerful source, and if the Froude Number is sufficiently high, the fire plume may take on the characteristics of a jet fire. The Froude Number is calculated using the following formula:

$$Q_d^* = \frac{\dot{Q}}{\rho_\infty c_p T_\infty D^2 \sqrt{gD}}$$

Where Q_d^* represents the Fire Froude number, which is non-dimensional, $\dot{Q}$ is the heat release rate, ρ_∞ represents the ambient density of air, c_p defines the specific heat, T_∞ represents the ambient temperature, D is the fire diameter, and g is the acceleration of gravity. The validation range is based on the peak heat release rate, so the peak heat release rate might also be used to compare the model application range to these values[24].

4.2 Flame Length Ratio

The flame length ratio quantifies the flame height in relation to the upper horizontal border (ceiling). The validation tests for NUREG-1824 all featured flames with a flame height at or below the ceiling. In cases when the flame height exceeds the roof, the flames will radiate outward from the point of impact[24].

$$\text{Flame Length Ratio} = \frac{H_f + L_f}{H_c}$$

Where H_f represents the base height of the fire, L_f represents the flame height, H_c is the enclosure height. Note that the flame length ratio does not apply to flames represented outside of an enclosure. The flame height is calculated using the following formula:

$$\frac{L_f}{D} = 3.7\ Q_d^{*\,2/5} - 1.02\ L_f$$

Where D represents the fire diameter, Q_d^* is the Fire Froude number.

4.3 Equivalence Ratio

This value represents the ratio of the fuel production rate to the oxygen supply rate. When the equivalency ratio is one, the appropriate quantity of oxygen necessary for total combustion is present. When the ratio is larger than one, the atmosphere is fuel-rich, and the fire is under-ventilated. When the ratio falls below one, the opposite is true. Estimating the equivalency ratio for natural and mechanical ventilation is possible using the equation:

$$\varphi = \frac{\dot{Q}}{\Delta H_{o_2} \dot{m}_{o_2}}$$

Where φ is the equivalence ratio, $\dot{Q}$ represents the heat release rate, ΔH_{o_2} is the heat of combustion for oxygen, and $\dot{m}_{o_2}$ is the mass flow rate of oxygen in the enclosure[24]. The following equation calculates the mass flow rate of oxygen into the enclosure:

$$\dot{m}_{o_2} = \begin{cases} 0.23 * \frac{1}{2} A_0 \sqrt{H_0}\ (\text{Natural Ventilation}) \\ 0.23\ \rho_\infty\ \dot{V}\ (\text{Mechanical Ventilation}) \end{cases}$$

Where A_0 is the effective area of the openings, H_0 represents the effective height of the openings, ρ_∞ represents the ambient density of air, and V is volumetric flow rate of air in the enclosure.

4.4 Compartment Aspect Ratio

The compartment aspect ratio is a way to measure how far from a cube the size of the enclosure is. When at least one of the compartment aspect ratios is high, the enclosure takes on corridor-like qualities. In such situations, the travel duration of the combustion products and a non-uniform layer might become essential characteristics that must be considered. When at least one of the compartment aspect ratios must be low for the enclosure to resemble a shaft. In such instances, stratification of the combustion products, the interaction between the fire plume and the enclosure borders, and blocked flow may become influential features[25]. The aspect ratio of a compartment is calculated using the following equation:

$$\text{Compartment Aspect Ratio} = \begin{cases} \frac{L}{H} \\ \frac{W}{H} \end{cases}$$

Where L represents the compartment's length, W represents its width, and H represents its height. The compartment aspect ratio is applicable when evaluating flames inside a room [25].

4.5 Radial Distance Ratio

The radial distance ratio is a measurement of the distance from the source fire's center at which a forecast heat flow amount may be determined. It only applies when the heat flux parameter is calculated. A low radial distance ratio implies that the target's

position is close to the fire and that the impacts of near-field thermal radiation might be severe. Large radial distance ratios indicate that the target is positioned at a considerable distance from the source of the fire[25]. The following equation gives the radial distance ratio:

$$\text{Radial Distance Ratio} = \frac{r}{D}$$

Where r represents the actual distance between the center of the firebase and the target, and D indicates the diameter of the fire[25]. In table-3 below, these values are calculated, and range intervals are specified according to NUREG-1824.

Table 3: Validation Parameters, Ranges, and Calculations

Quantity	Formula	Validation Range	Calculations For 464 and 1002 Kw HRR
Fire Froude Number	$Q_d^* = \frac{\dot{Q}}{\rho_\infty c_p T_\infty D^2 \sqrt{gD}}$	0.4 – 2.4	1.009 – 1.171
Flame Length Ratio	$\frac{L_f}{D} = 3.7\, Q_d^{*\frac{2}{5}} - 1.02$ $\frac{H_f + L_f}{H_c}$	0.2 – 1.0	0.704 – 0.824
Equivalence Ratio	$\varphi = \frac{\dot{Q}}{\Delta H_{o_2} \dot{m}_{o_2}}$ $\dot{m}_{o_2} = \begin{cases} 0.23 * \frac{1}{2} A_0 \sqrt{H_0}\ (\text{Natural Ventilation}) \\ 0.23\, \rho_\infty\, \dot{V}\ (\text{Mechanical Ventilation}) \end{cases}$	0.04 – 0.6	0.088 – 0.198
Compartment Aspect Ratio	$\frac{L}{H}$ or $\frac{W}{H}$	0.6 – 5.7	4.35 and 3.03
Radial Distance Ratio	$\frac{r}{D}$	2.2 – 5.7	2.2

Chapter 5 Model and Simulation Results

Construction

The switchgear room to be analyzed has three electrical cabinets, and there are nine cable trays above each electrical cabinet. The plan and design of the Switchgear room are shown in figure 10.

The size of the switchgear room is 27.5m X 19.5m X 7.1 m. The room ceiling, floor, and walls are concrete, and the thickness of these walls is 0.5 m. Cable trays and cabinets are made of steel. The cabinets are 1 m wide, 18.5 m long, and 2.4 m high, as seen in Figure 10. The thickness of the cabinet housings is 1.5 mm. The trays are 0.8 m wide, 24.5 m long, and 0.1m high. The thickness of the steel cable trays is 3 mm, as seen in Figure 11.

Meshes

Only one mesh is used in the model. The mesh alignment test is passed. The characteristic fire diameter "D*" is calculated as 0.705 m by using the fire diameter formula. According to the FDS User Guide NUREG 1824, a "D*/dx" ratio is recommended between 4 and 16 to resolve fires in various scenarios accurately. According to this ratio, the grid size (dx) is calculated at around 0.16m. The total number of cells for this mesh is 923,296, as seen in Figure 12.

Ventilation

As illustrated in Figure 13, three return and three supply vents are placed along the side walls. Each vent measures 0.5 m by 0.6 m and has a 0.47 m3/s airflow rate. It is assumed that the mechanical ventilation is turned on during the fire, and regular activities

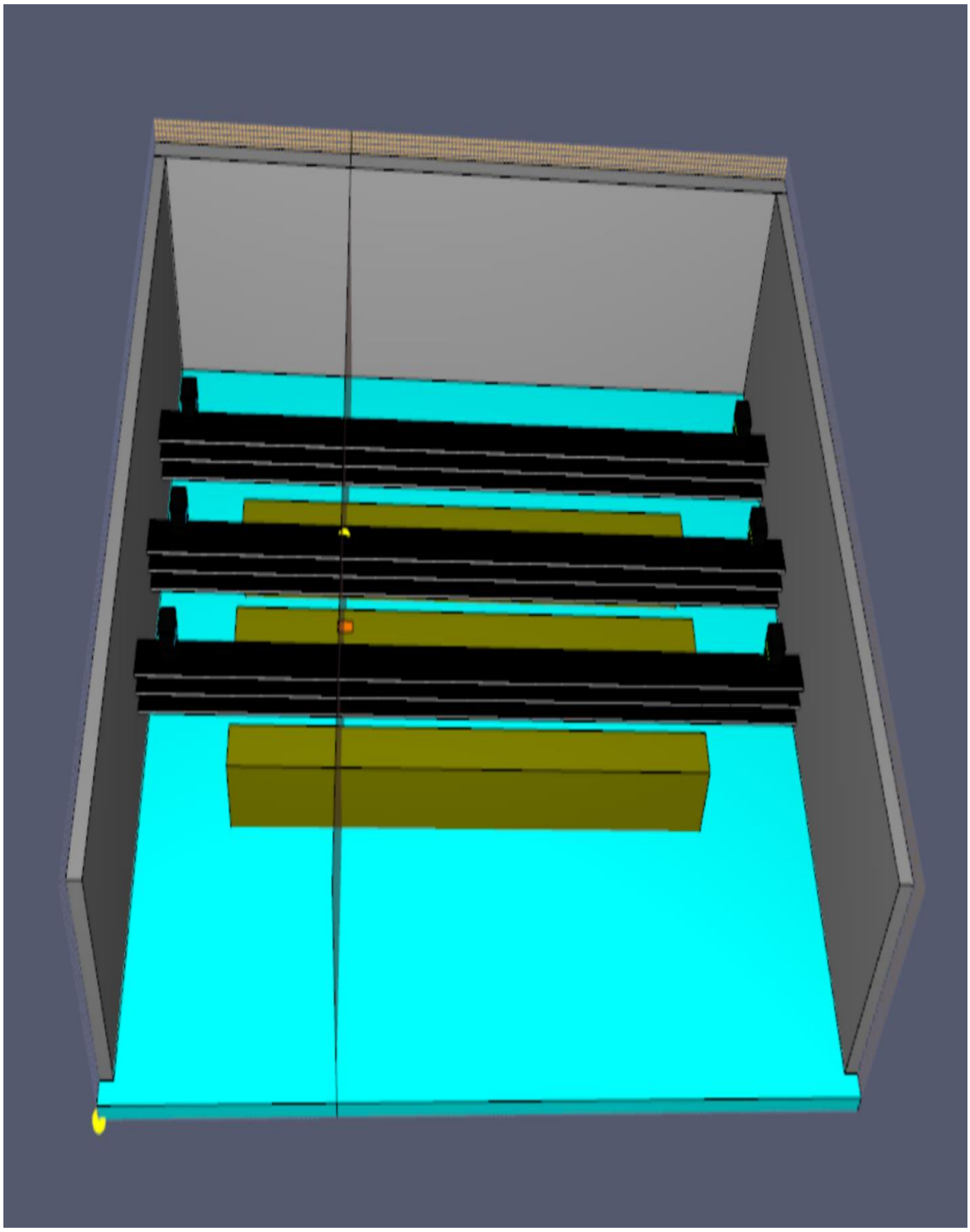

Figure 10: The switchgear room's geometry.

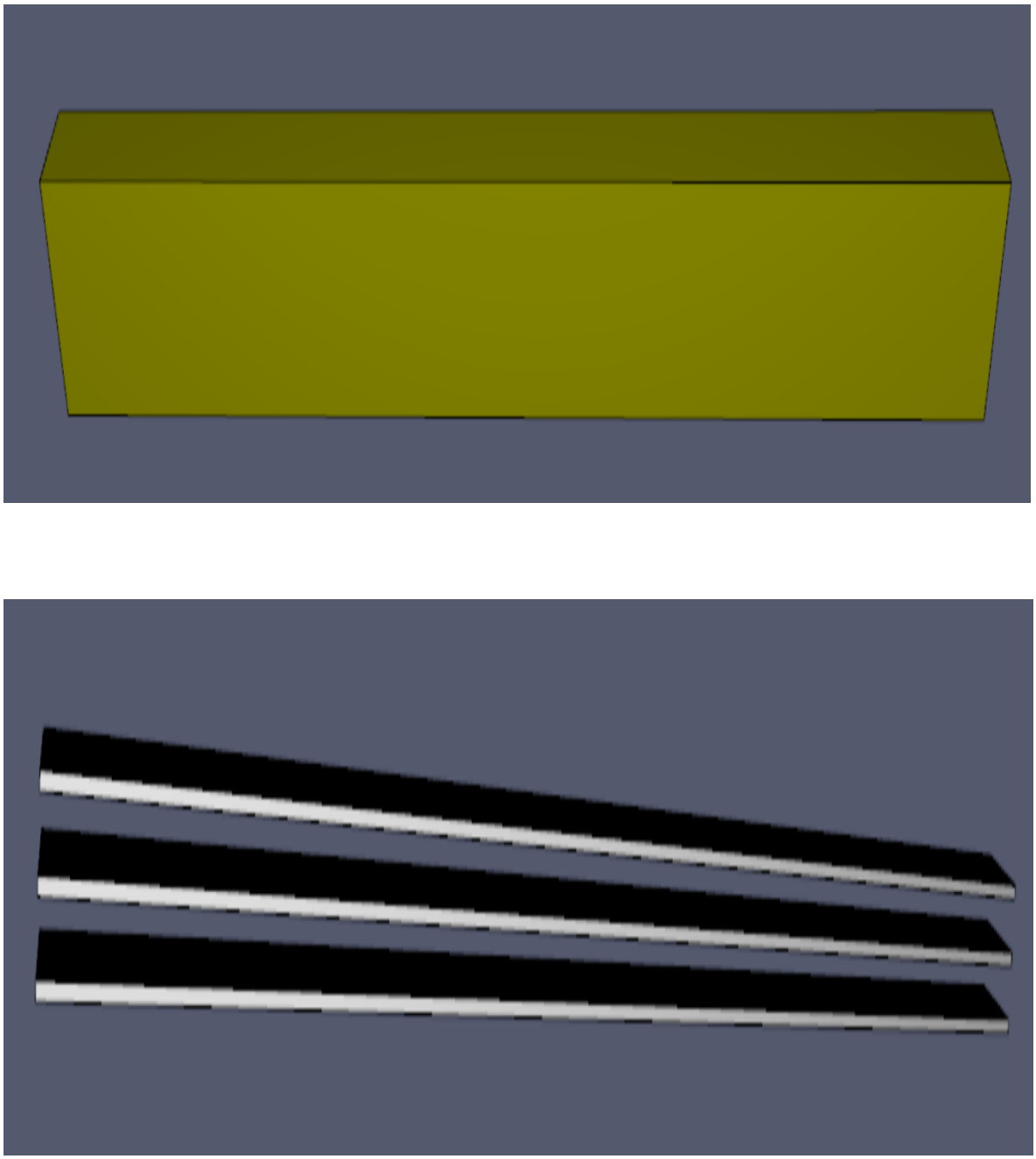

Figure 11: Cabinets and cable trays.

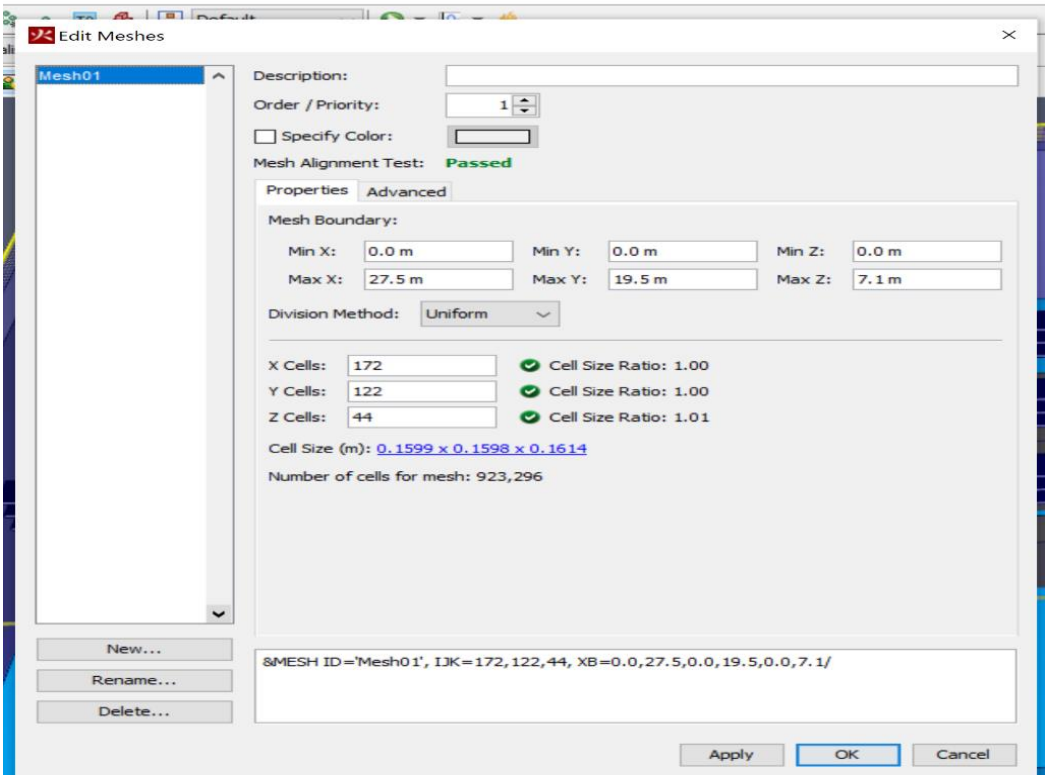

Figure 12: Meshes description.

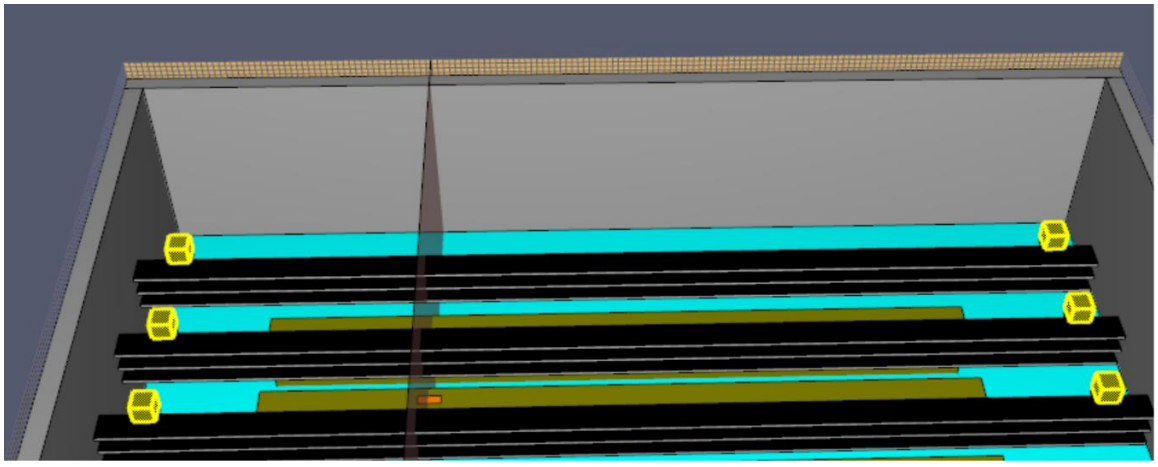

Figure 13: Supply and return vents

continued. The supply vents get the same amount of air from the room, and the return vents get the same amount of air from the room. The temperature in the switchgear room is 20 °C (68 °F).

Also, the top of the middle cabinet has a vent for air. This vent is 0.6 m in width and 0.3 m in length. The height of the cabinet is 2.4 m. According to the NUREG/CR-6850, the fire burns within the cabinet's interior. By placing such a vent on the cabinet, the heat, smoke, and perhaps flames exhaust through the vent at the cabinet's top, which means that the initial fire source. That is, this vent is intended to symbolize a fire that burns towards the cabinet's top and exits through the use of the vent.

A model based on actual data assumes that the angle of horizontal spread from tray level to tray level is $35°$ on each side. The $35°$ angle of fire spread is based on the results of a fire test that used 14 filled horizontal cable trays in an array that was two trays wide and seven trays high[13]. The formula below describes the lateral extent of the burning cable in higher trays before the start of lateral spread.

$$L_i = L_{i-1} + 2h_i \tan 35°$$

Where "L_i" represents the length of tray "i," and "h_i" is the distance from bottom to bottom. Figure 14 shows the model. The vent is 0.8 meters wide and 0.6 meters long in the first cable tray. Using the formula, the calculated vent is 0.8 meters wide and 1.4 meters long in the second cable tray. The vent in the third cable tray is 0.8 meters wide and 2 meters long, as shown in Figure 14.

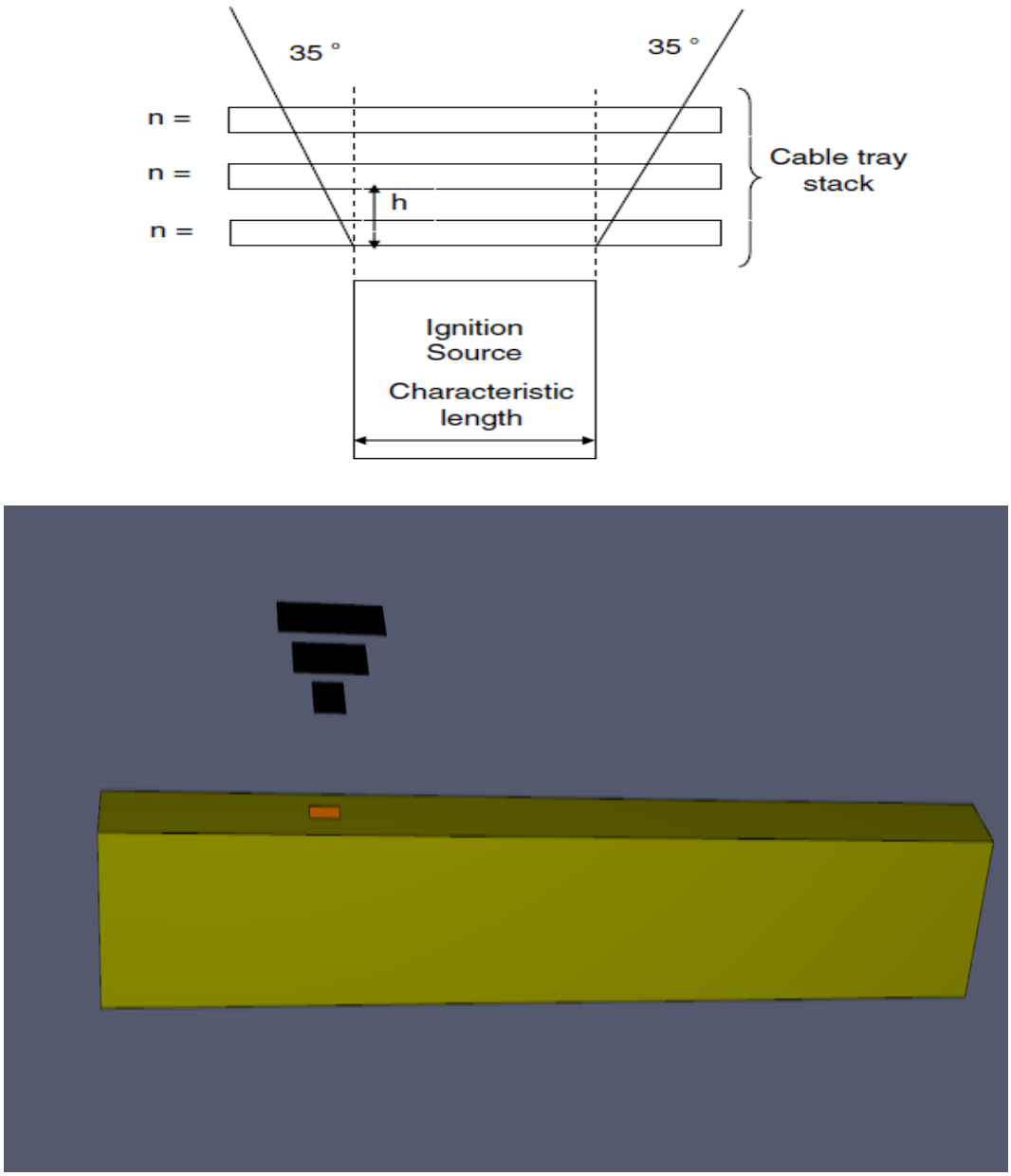

Figure 14: Model of Fire Spread in the Cable Tray

Fire

The fire is ignited in the middle cabinet. Two different 464 kW and 1002 kW heat release rates (HRR) were used in the switchgear room. This fire vent is 0.6 m in width and 0.3 m in length for these two scenarios. The heat release rate per area (HRRPUA) for both scenarios are calculated as around 2578kW/m2 and 5566 kW/m^2.

For these different two scenarios, t-squared (t^2) fire ramp times are calculated by using the $Q = \alpha t^2$, where "Q" represents the HRR (kW), "α" is the fire growth rate coefficient (kW/s^2), and "t" is time (s).

The time is calculated as 398 and 585 seconds for 464 and 1002 kW HRR, respectively, by selecting the slow alpha coefficient of 0.00293 (kW/s^2) in table-4. These calculated ramp-up times and heat release rate per area (HRRPUA) values were created by creating a fire surface in the PyroSim software for both scenarios, as seen in Figure 16.

According to NUREG/1805, if the temperature of the cables reaches around 205 °C, the cables begin to burn and become damaged. There is a Gas or Solid Phase Device section in the PyroSim program. These devices measure values in the gas and solid phases in this section. 205 °C enable setpoint is set as seen in Figure 17.

To use the simulation output, there is a 2D slices section available in the PyroSim program. 2D Slices measure gas-phase data such as pressure, velocity, and temperature on an axis-aligned plane. The 3D Results can then be used to animate and show this data. A 2D slice is placed on the 8.3 m X-axis, which passes through the center of the fire to see temperature values, as seen in Figure 18.

Table 4: Fire growth rate coefficients

Standard Alpha Values (kW/s^2)	
Slow	0.00293
Medium	0.01172
Fast	0.0469
Ultrafast	0.1876

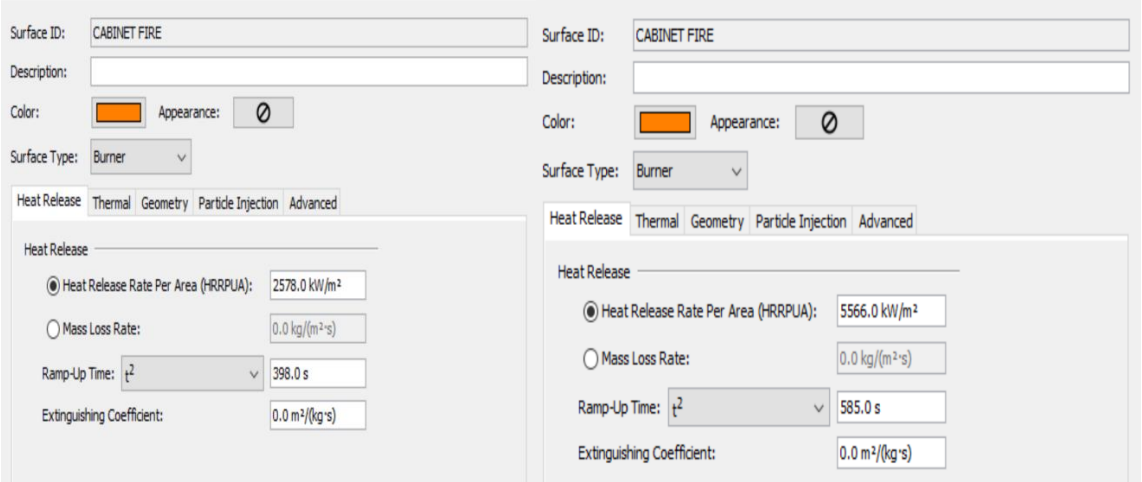

Figure 15: Cabinet Fires Values

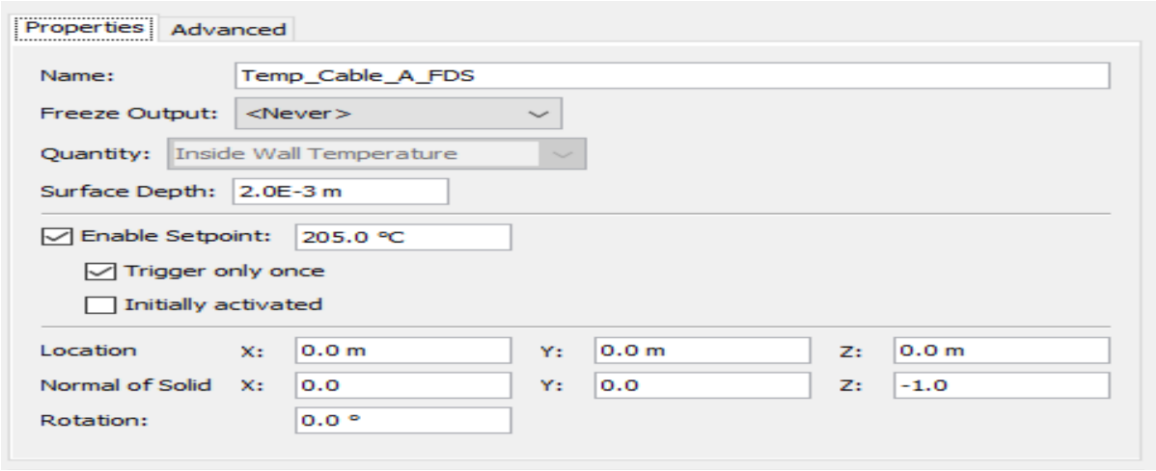

Figure 16: Temperature Devices Setpoint

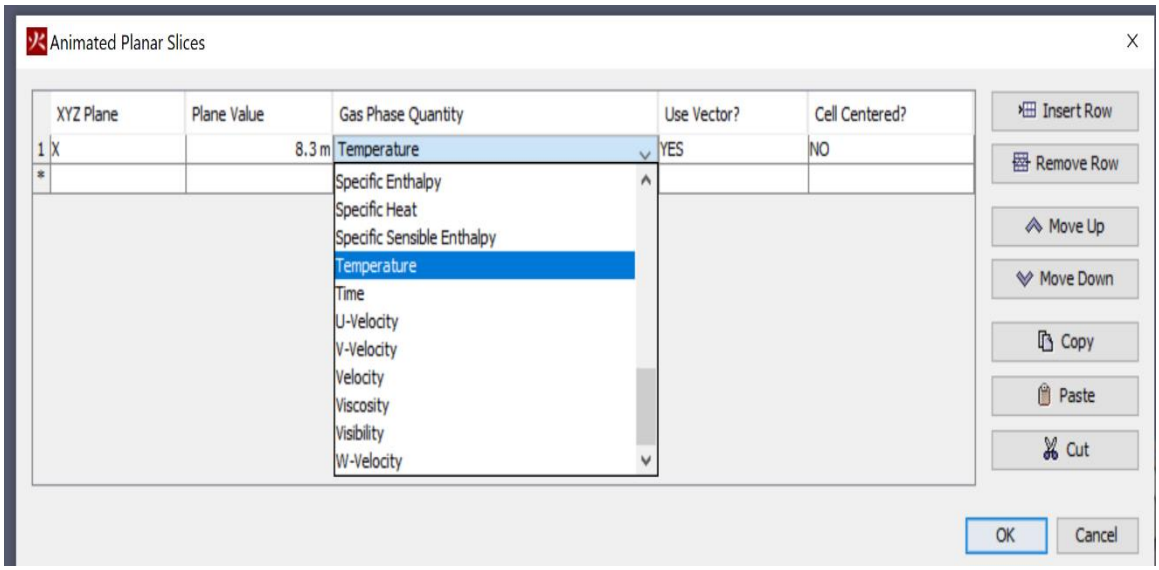

Figure 17: 2D Slice

The time is calculated as 398 and 585 seconds for 464 and 1002 kW HRR, respectively, by selecting the slow alpha coefficient of 0.00293 (kW/s^2) as shown Figure 19.

In the first cable tray, the peak temperature measured for 464 kW HRR is around 445, while this value is around 695 for 1002 kW HRR. In this cable tray, the ignition time is determined as about 606 seconds for 464 kW HRR, while it is determined as about 504 seconds for 1002 kW HRR as shown Figure 20.

In the second cable tray, the ignition time is determined as around 684 seconds for 464 kW HRR, while it is determined as about 600 seconds for 1002 kW HRR as shown Figure 21.

In the third cable tray, the ignition time is determined as around 875 seconds for 464 kW HRR, while it is determined as about 750 seconds for 1002 kW HRR as shown Figure 22.

In the side cabinets, the peak temperature measured for 464 kW HRR is around 130, while this value is around 170 for 1002 kW HRR. This means that since the temperature in these side cabinets did not reach the critical value of 205 thresholds, the fire did not occur as shown Figure 23.

At the same time, the peak heat flux value for 464 kW HRR was measured as 4 in these side cabinets, while this value was 6.5 for 1002 kW HRR as shown Figure 24.

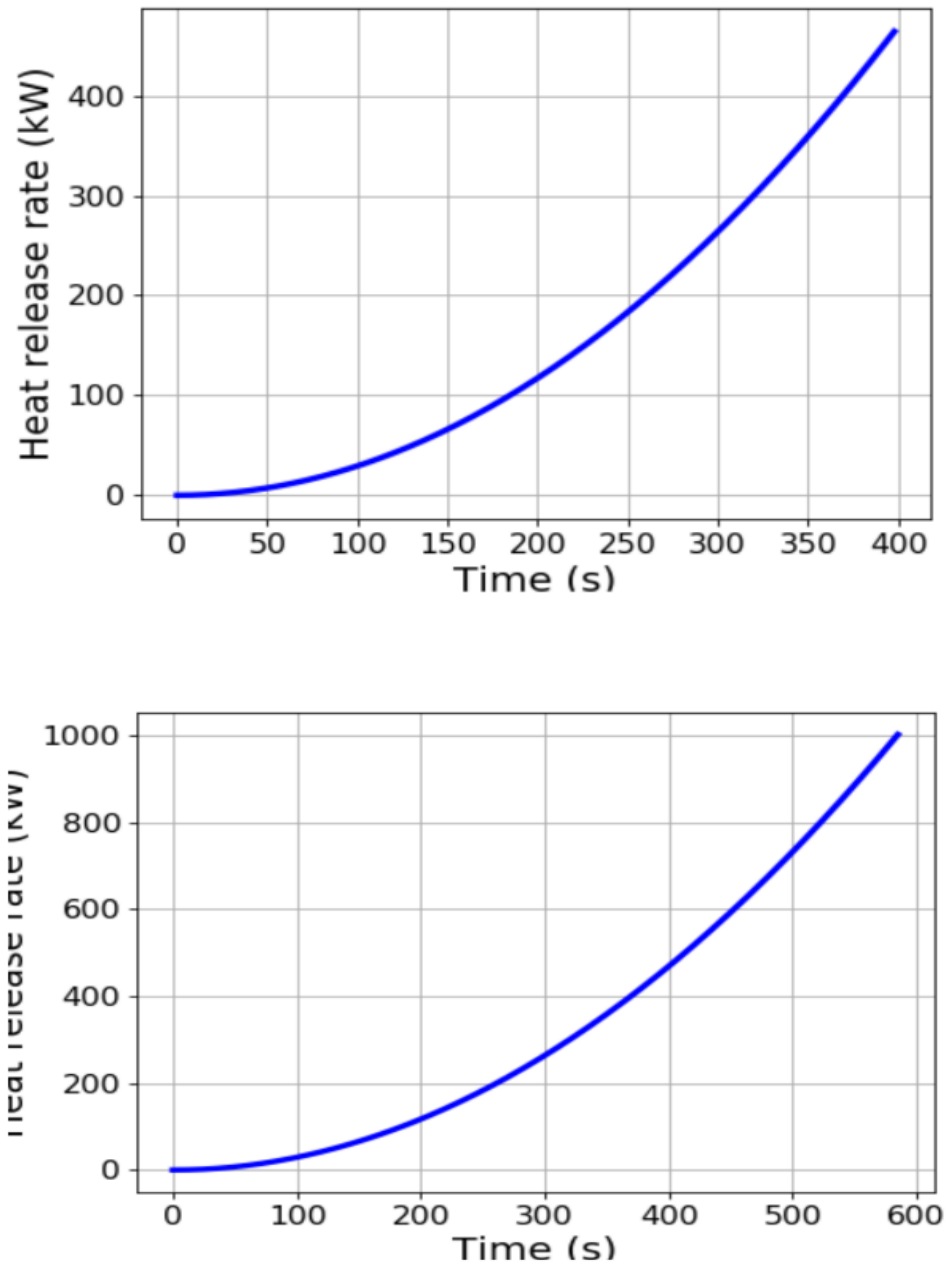

Figure 18: The heat release rates for different fire scenarios 464 kW and 1002 kW, respectively

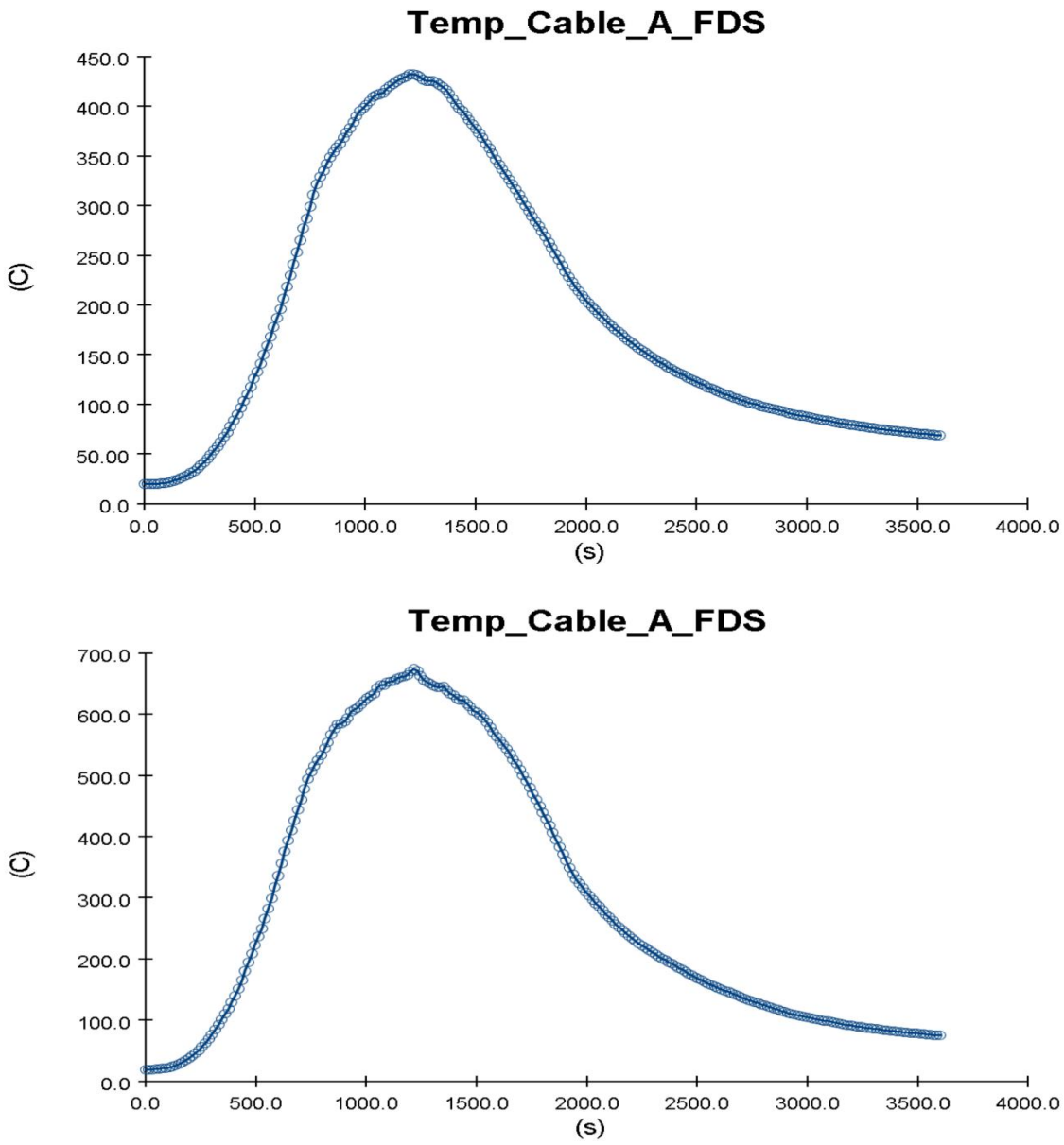

Figure 19: The temperature for different fire scenarios 464 kW and 1002 kW, respectively, in the first cable tray

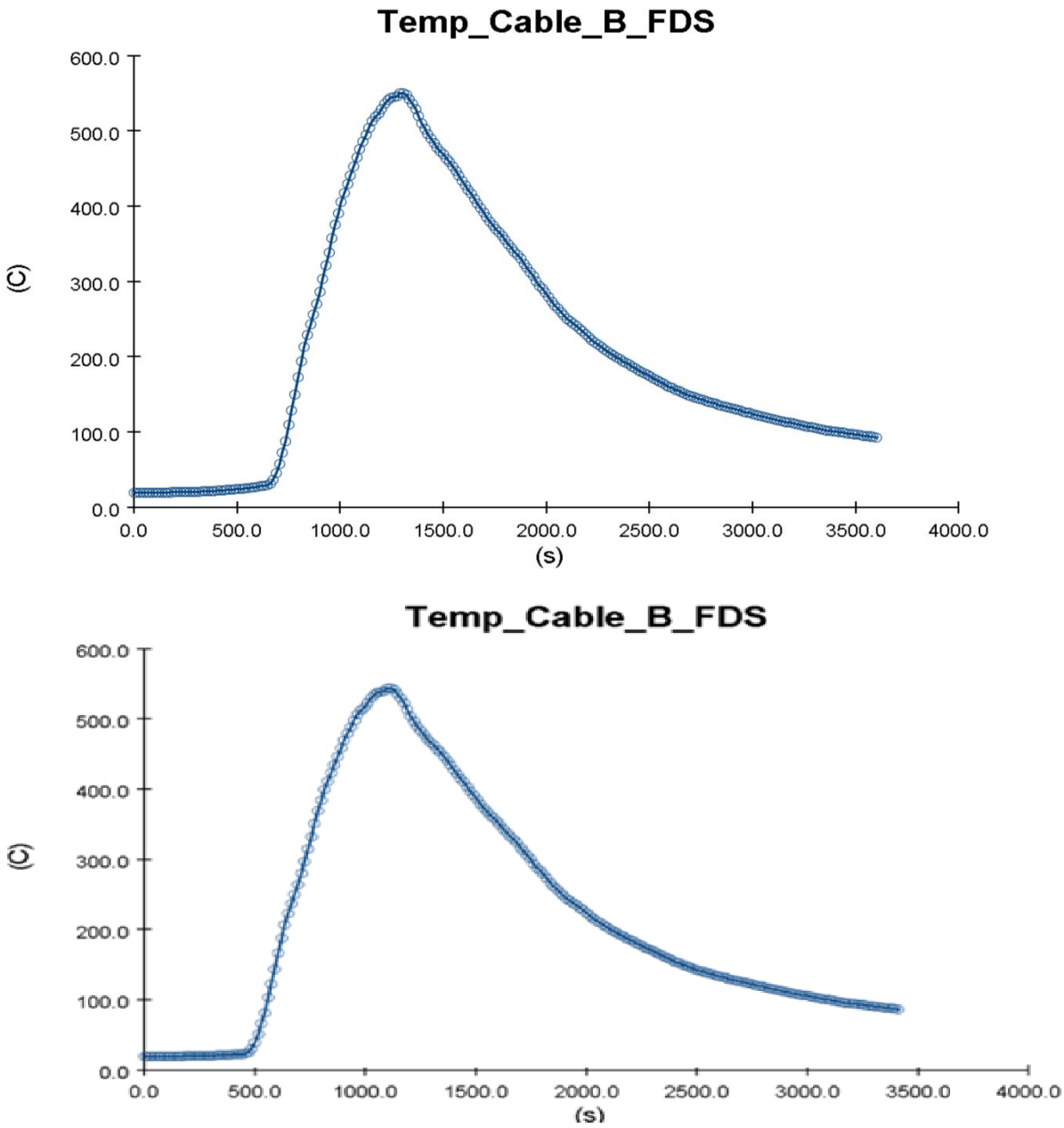

Figure 20: The temperature for different fire scenarios 464 kW and 1002 kW, respectively, in the middle cable tray

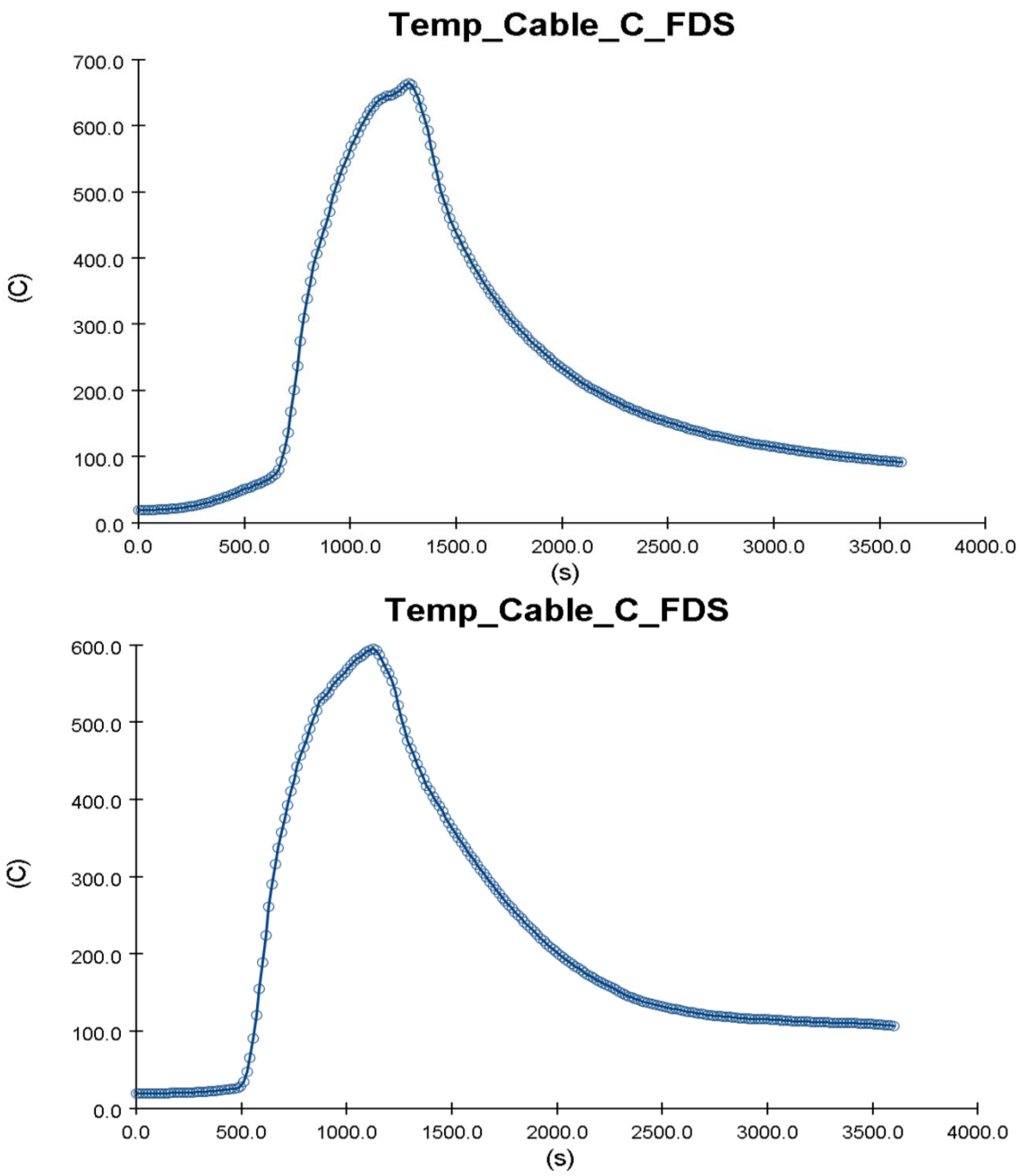

Figure 21: The temperature for different fire scenarios 464 kW and 1002 kW, respectively, in the third cable tray

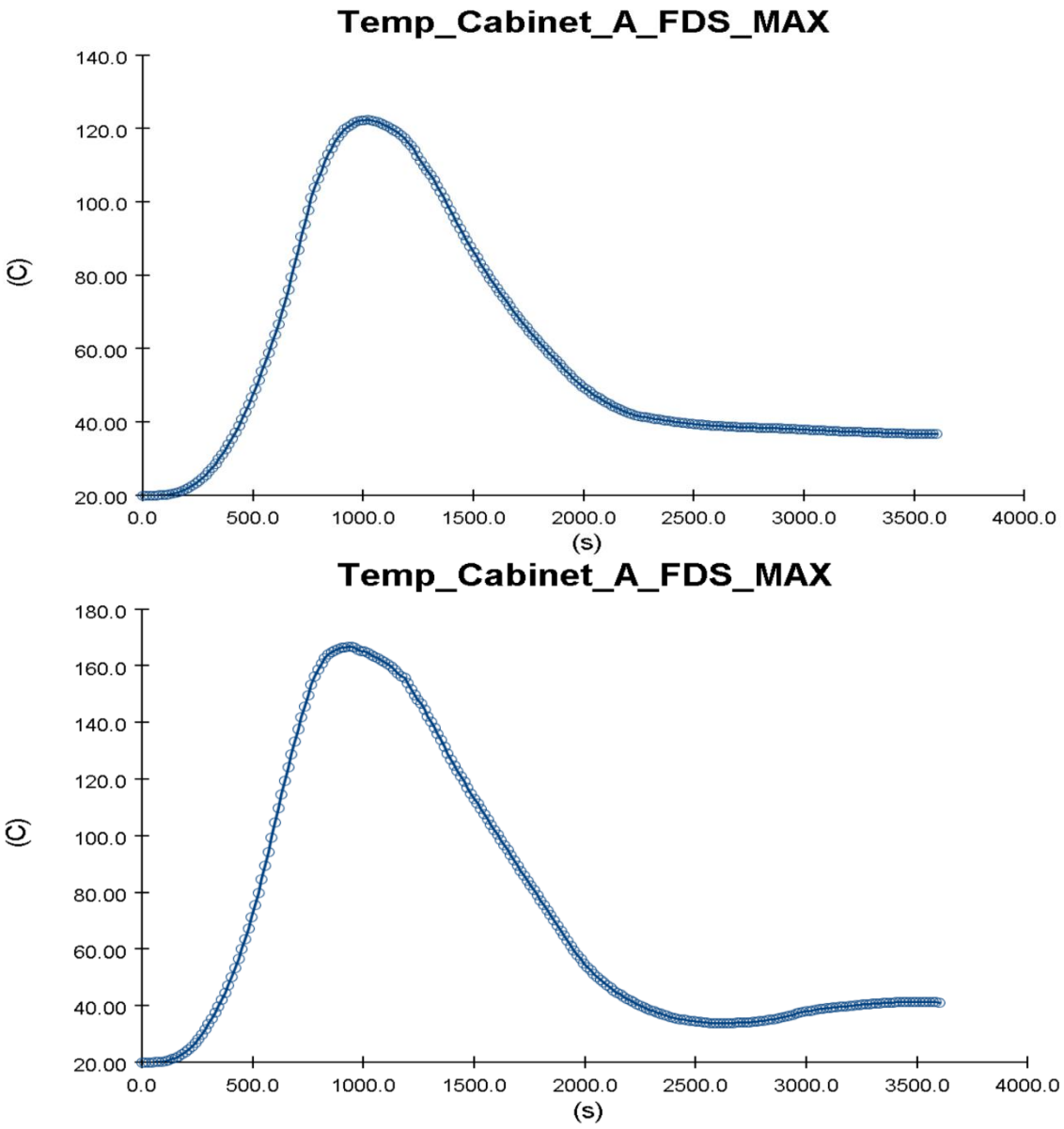

Figure 22: The temperature for different fire scenarios 464 kW and 1002 kW, respectively, in the side cabinets

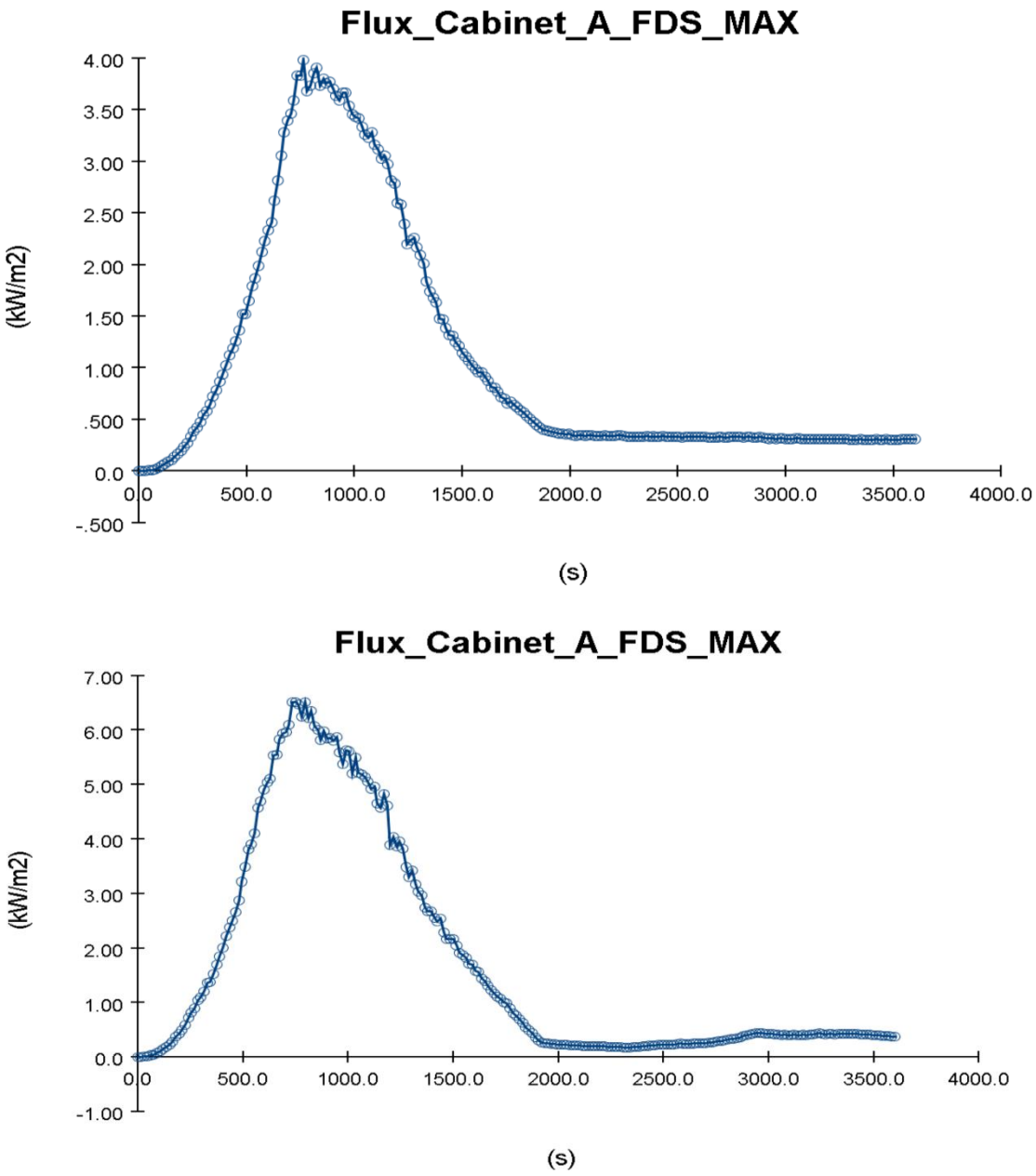

Figure 23: The heat flux for different fire scenarios 464 kW and 1002 kW, respectively, in the side cabinets

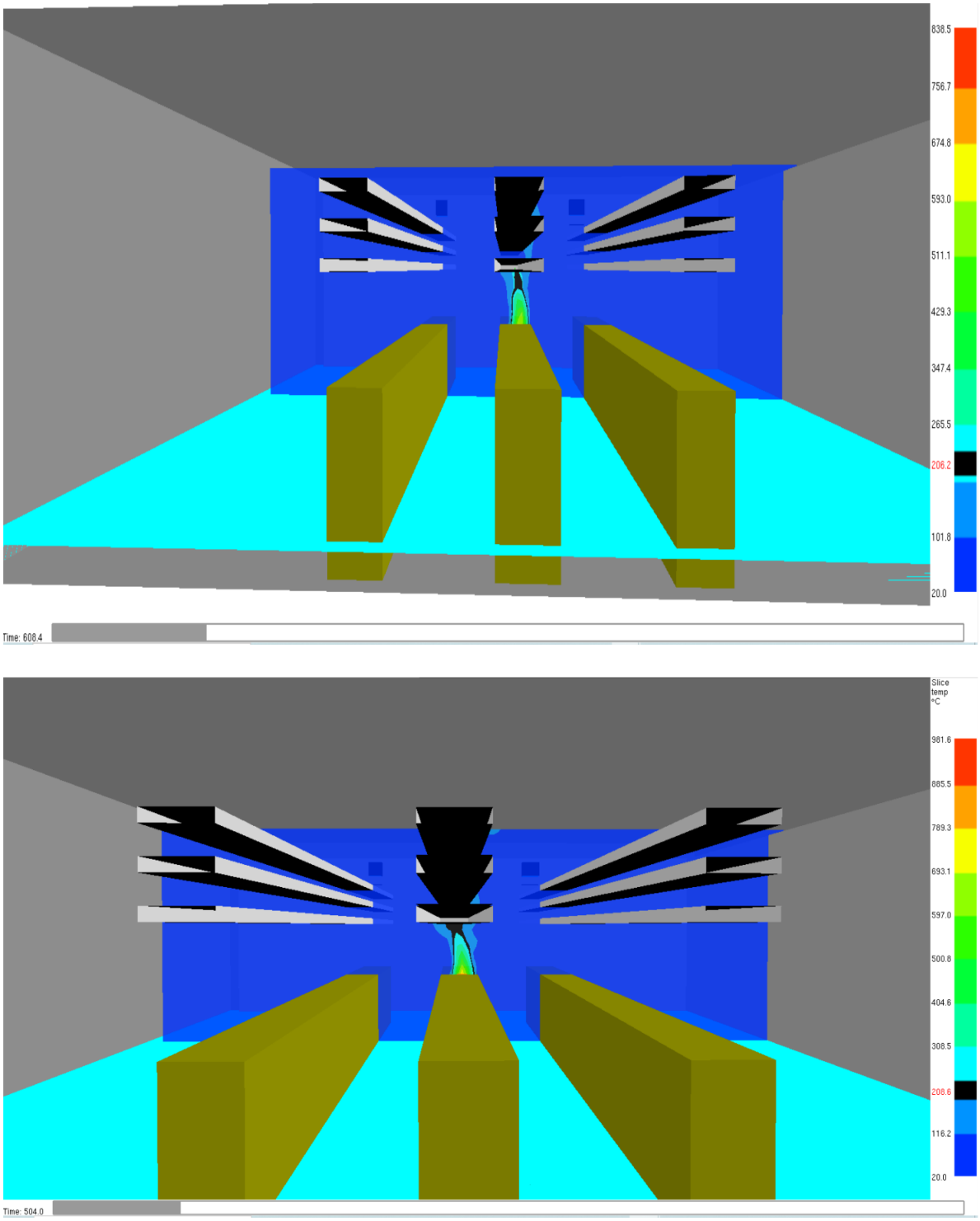

Figure 24: The ignition time for different fire scenarios 464 Kw and 1002 kW, respectively, in the first cable tray by using the Smokeview (SMV) program

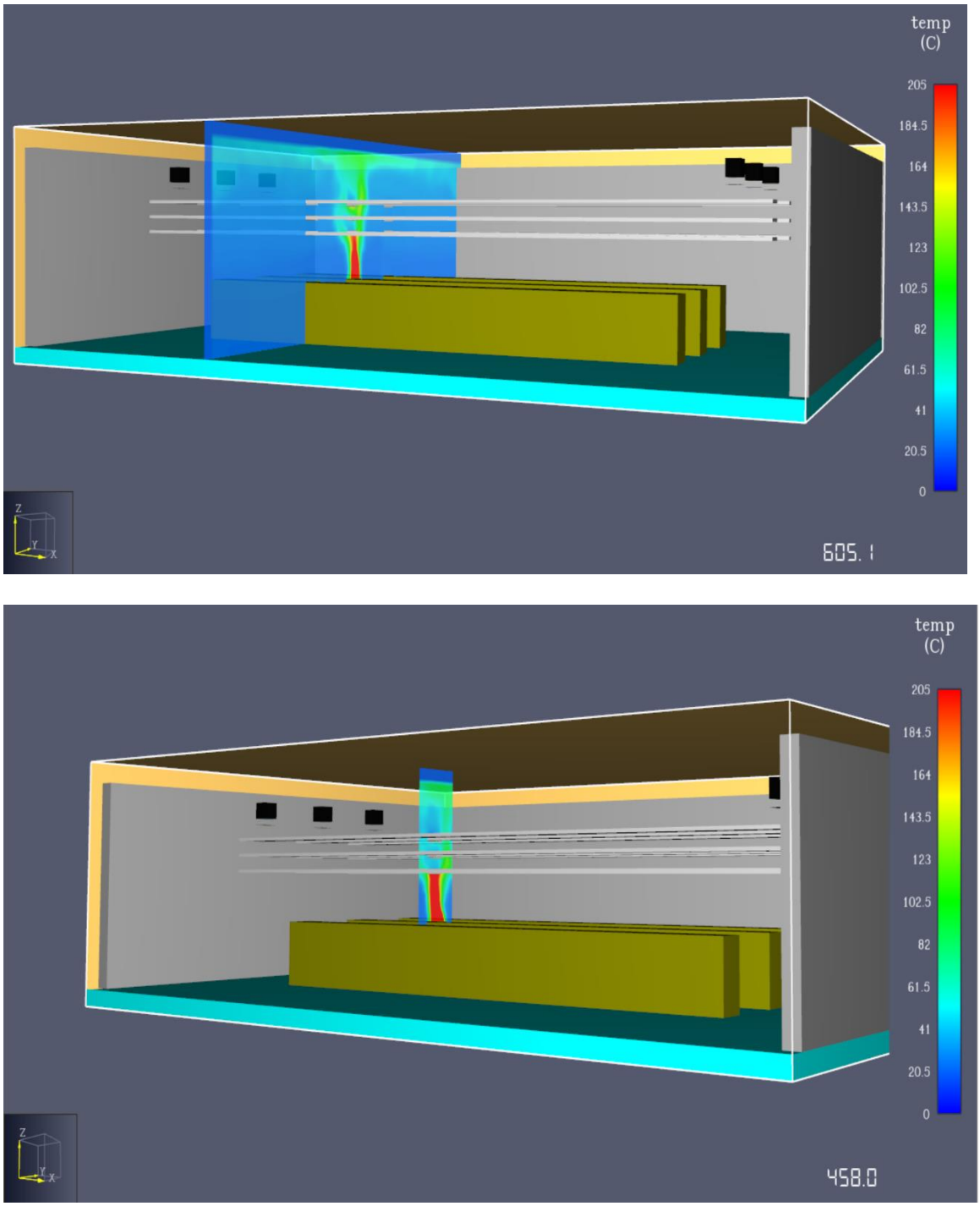

Figure 25: The ignition time for different fire scenarios 464 kW and 1002 kW, respectively, in the first cable tray by using the PyroSim program

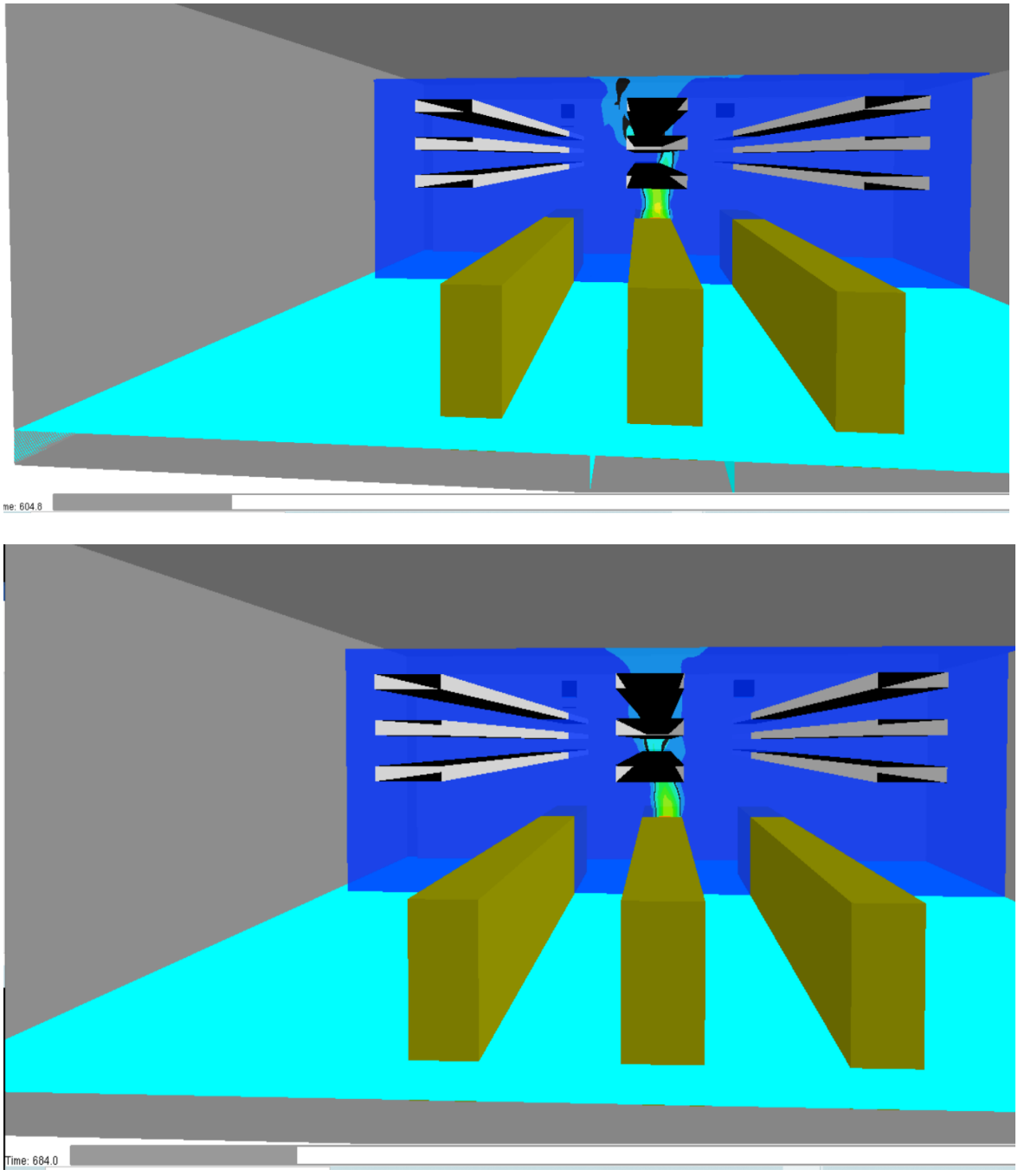

Figure 26: The ignition time for different fire scenarios 464 kW and 1002 kW, respectively, in the second cable tray by using the Smokeview (SMV) program

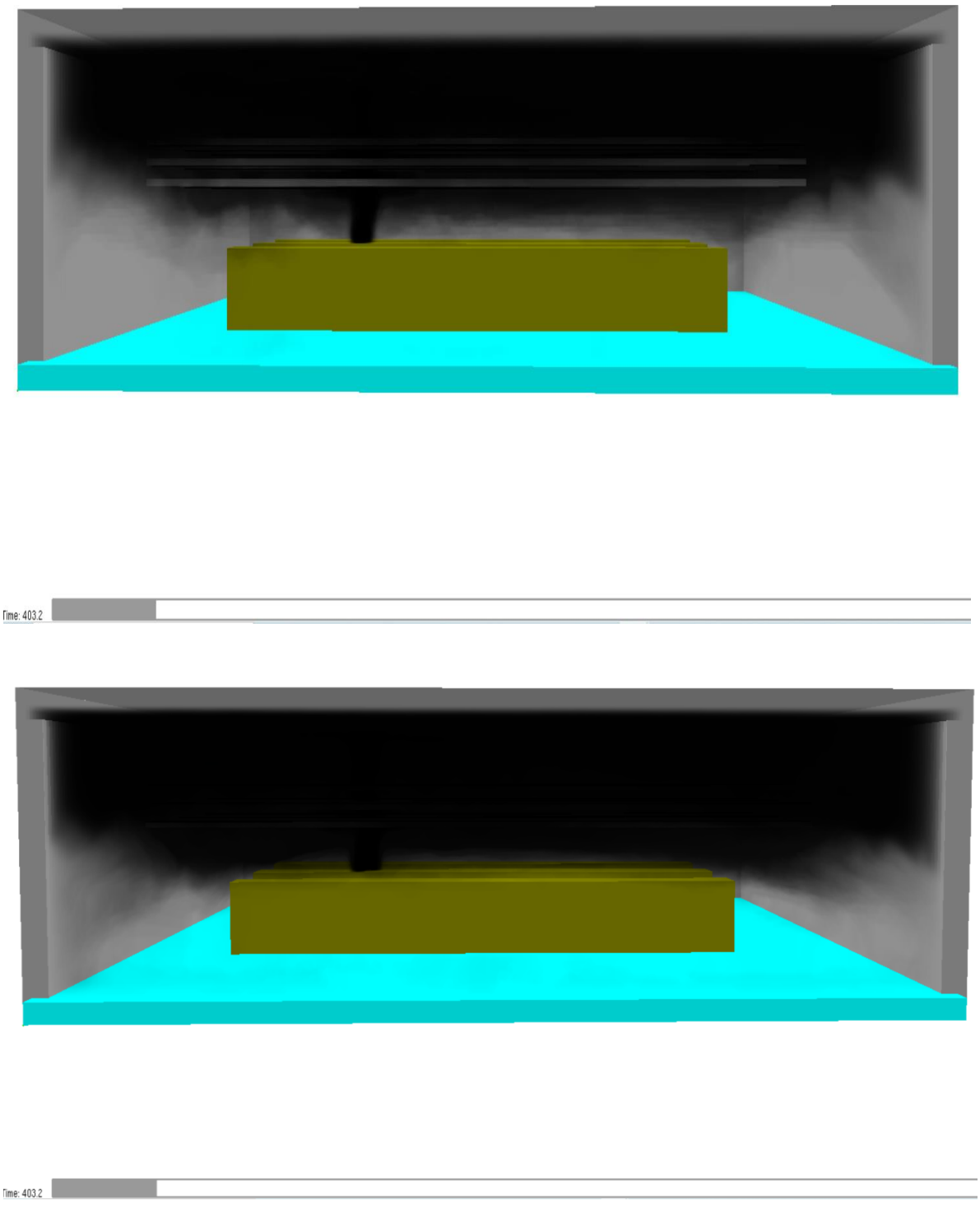

Figure 27: Soot density for 464 and 1002 kW in 403s.

Table 5: Summary of the model switchgear room results of fire.

HRR (kW)	Target	Ignition Time (s)	Critical Temperature Value (°C)
Temperature			
464	First Cable Tray	606	205
1002		504	205
464	Second Cable Tray	684	205
1002		604	205
464	Third Cable Tray	875	205
1002		743	205
464	Side Cabinets	No	205
1002		No	205
Heat Flux (kW/m^2)			
464	Side Cabinets	4	7
1002		6.5	7

CHAPTER 6 CONCLUSION AND FUTURE WORK

Nuclear safety is essential for efficiently managing radioactive emissions into the atmosphere. Fires at nuclear power facilities represent a substantial risk to nuclear safety, based on past experience. Switchgear rooms at nuclear power reactors are one of the places where fires commonly occur, and it is difficult to put the fire out when one happens. The primary cause of these fires is the installation of many cables in these locations, such as cable trays and cabinets. The materials of electrical cables can lead to the spread of fire. This analysis determined whether a possible fire in a cabinet in the switchgear room caused a fire in the cable trays located horizontally above the cabinets and in other cabinets and its duration. 464 kW and 1002 kW heat release rates (HRR) values were used for the fire. It has been modeled and simulated in the Pyrosim program, which uses the computational fluid dynamic (CFD) fire model because this model gives more detailed and accurate simulation results. According to the simulation results, the fire ignites the cables in the first cable trays close to the cabinet after about 10 minutes for 464 kW HRR, while this time for 1002 kW HRR was around 8 minutes. Then, ignition started at different times in the second and third cable trays, respectively. Based on the failure threshold of 205 °C (420F) for the general thermoplastic cable class, this model was made, and the simulation was run. Since the critical values of 205 °C (420F) and 7 kW/m^2heat flux did not exceed both HRR values in the side cabinets, so ignition did not occur. As a result, because of the fire that occurred in the cabinet, it is anticipated that there will be a second fire in the cable trays. There are approximately 10 minutes to protect this second additional fire.

Nuclear power reactors are built and licensed to provide energy reliably and safely for at least 40 years. In future studies, it can be determined how long the fire will cause the second fire in these cable trays by placing fire barriers between these cable trays.

REFERENCES

[1] K. Mcgrattan and S. Hostikka, "Verification and Validation Process of a Fire Model".

[2] Dennis L. Berry, Nuclear Power Plant Fire Protection Philosophy and Analysis. 1980. Accessed: May 18, 2022. [Online]. Available: https://www.osti.gov/servlets/purl/5192225

[3] A. Matsuda, "Fire safety simulation of cable fire in nuclear power plant room based on flammability database of cables."

[4] "Introduction to fire safety in nuclear power plants," 1991.

[5] E. M. Project Manager H Salley RP Kassawara, "Verification & Validation of Selected Fire Models for Nuclear Power Plant Applications," 2007.

[6] M. H. Jee, C. K. Moon, and H. T. Kim, "Performance-based firefighting strategies for confined fire zones in nuclear power plants," Progress in Nuclear Energy, vol. 62, pp. 16–25, Jan. 2013, doi: 10.1016/j.pnucene.2012.08.001.

[7] "Fire Protection in Nuclear Power Plants."

[8] "NUREG 1805 Fire dynamics tools".

[9] U. S. Nuclear, "NUREG-1934, 'Nuclear Power Plant Fire Modeling Analysis Guidelines (NPP FIRE MAG),' Final Report." [Online]. Available: http://www.nrc.gov/reading-rm.html.

[10] U. S. Nuclear, "NUREG-1934, 'Nuclear Power Plant Fire Modeling Analysis Guidelines (NPP FIRE MAG),' Final Report." [Online]. Available: http://www.nrc.gov/reading-rm.html.

[11] "Experience gained from fires in nuclear power plants: Lessons learned," 2004, Accessed: May 18, 2022. [Online]. Available: http://www-ns.iaea.org/standards/

[12] J. W. Brown, S. P. Nowlen, and F. J. Wyant, "SANDIA REPORT High Energy Arcing Fault Fires in Switchgear Equipment, A Literature Review." [Online]. Available: http://www.ntis.gov/help/ordermethods.asp?loc=7-4-0#online

[13] Epri, "EPRI/NRC-RES Fire PRA Methodology for Nuclear Power Facilities Volume 2: Detailed Methodology Final Report," 1989. [Online]. Available: http://www.nrc.gov/reading-rm.html.

[14] F. Bonte, N. Noterman, and B. Merci, "Computer simulations to study interaction between burning rates and pressure variations in confined enclosure fires," Fire Safety Journal, vol. 62, no. PART B. Elsevier Ltd, pp. 125–143, 2013. doi: 10.1016/j.firesaf.2013.01.030.

[15] A. Matsuda, "Fire safety simulation of cable fire in nuclear power plant room based on flammability database of cables."

[16] "Fire Protection in Nuclear Power Plants".

[17] K. Han, I. Kang, and H. G. Lim, "Multi-compartment Fire Modeling for Switchgear Room using CFAST."

[18] M. H. Salley and R. P. Kassawara, "Verification & Validation of Selected Fire Models for Nuclear Power Plant Applications Volume 6: Fire Dynamics Simulator," 2006.

[19] "PyroSim - User Manual."

[20] "PyroSim - Results User Manual."

[21] R. Lofaro et al., "Literature Review of Environmental Qualification of Safety-Related Electric Cables Literature Analysis and Appendices."

[22] P. Rantuch, T. Štefko, and J. Martinka, "Critical Heat Flux Determination of Electric Cable Insulation," Research Papers Faculty of Materials Science and Technology Slovak University of Technology, vol. 26, no. 42, pp. 11–20, Jun. 2018, doi: 10.2478/rput-2018-0001.

[23] David, "Cable Heat Release, Ignition, and Spread in Tray Installations During Fire (CHRISTIFIRE) Phase 1: Horizontal Trays." [Online]. Available: http://www.nrc.gov/reading-rm.html.

[24] E. Power, "Verification and Validation of Selected Fire Models for Nuclear Power Plant Applications Volume 3: Fire Dynamics Tools (FDTS)." [Online]. Available: http://www.nrc.gov/reading-rm/doc-collections/nuregs

[25] K. Mcgrattan and S. Hostikka, "Verification and Validation Process of a Fire Model."

VITA

Yalcin Meraki was born in Ankara, TURKEY. He attended Erciyes University and graduated from Mechanical Engineering Department in 2012. After graduating his bachelor's degree, he has worked in private sector for 4 years. During his private working life, Yalcin got a scholarship which is provided by the Turkish Ministry of National Education. He attended the University of Tennessee Knoxville in 2020.